Impacts of Salinity and Seasonality on Reproductive Physiology in Diploid and Tetraploid Eastern Oyster (*Crassostrea virginica*)

by

Victoria MacKenzie Tackett

A thesis submitted to the Graduate Faculty of
Auburn University
in partial fulfillment of the
requirements for the Degree of
Master of Science

Auburn, Alabama
December 9, 2023

Keywords: Broodstock, Egg quality, Reproduction, Sperm quality, Triploid

Approved by
Ian A.E Butts, Chair, Associate Professor of Fisheries, Aquaculture, and Aquatic Science
James A. Stoeckel, Associate Professor of Fisheries, Aquaculture, and Aquatic Science
Andrea M. Tarnecki, Assistant Extension Professor of Fisheries, Aquaculture, and Aquatic Science

Abstract

The demand for high-value aquaculture products, like Eastern oyster (*Crassostrea virginica*), necessitates efficient commercial hatchery strategies. Triploid oysters, derived from mating diploid females with tetraploid males, exhibit enhanced growth and meat quality. However, challenges in triploid production persist due to various factors, particularly low gamete quality. This thesis investigated the influence of salinity on gamete quality in Eastern oyster and provided a comprehensive assessment of male tetraploid and female diploid gametogenesis and gamete quality over the annual cycle. Lower salinities negatively impacted most sperm traits while higher salinity increased lipid peroxidation and egg irregularities. Gamete quantity and quality varied annually with all sperm traits displaying peak performance in June and July. High-quality oocytes were also produced in June and July. These findings emphasize the importance of salinity and season in gamete quality and offer novel insights for optimizing the aquaculture of Eastern oyster in the Gulf of Mexico.

Acknowledgments

While there are countless people to thank for their help during this project, I am deeply grateful to my advisor, Dr. Ian A. E. Butts, whose guidance, support, and encouragement was invaluable throughout this research. His expertise, patience, and unwavering commitment have been instrumental in shaping this thesis. Not to mention the invaluable statistical support. I would like to express my sincere appreciation to the members of my thesis committee, Dr. Jim A. Stoeckel and Dr. Andrea M. Tarnecki, for their insightful feedback and constructive criticism that greatly enhanced the quality of this work. Additionally, I would like to thank all the Reproductive Physiology Lab members for their help during this thesis. My heartfelt thanks go to the Auburn University Shellfish lab on Dauphin Island, who maintained, cleaned, and shipped the oysters used during this study. This project would not have been possible without the hard work and expertise provided by Scott Rikard and Sarah Spellman, Christina LoBuglio, Kayla Boyd and Meghan Capps. Special thanks to boat captain Kevin Landry for collecting the oysters used in this experiment.

Tyler, thank you for the countless hours of support. I would not have been able to maintain my sanity without you. Your love and belief in my abilities have been a source of strength.

Most importantly I would like to thank my parents, Dorrie and Jay Tackett, for their unwavering understanding, support, and encouragement during my academic journey. While my mom was not with me to experience this phase of my life, I would not be the scientist or person I am today without her and my dad's guidance.

Table of Contents

List of Figures

List of Tables

List of Abreviations

ARPL	Aquatic Reproduction Physiology Lab	MDA	Malondialdehyde
ASW	Artificial Salt Water	MUFA	Monounsaturated fatty acids
ATP	Adenosine 5'-triphosphate	OMI	Oogonia Maturity Index
AUSL	Auburn University Shellfish Lab	PPT	Parts Per Thousand
CASA	Computer Assisted Sperm Analysis	PSU	Practical salinity unit
CV	Coefficient of Variation	PUFA	Polyunsaturated fatty acids
DHA	Docosahexaenoic acid	RAS	Recirculating Aquaculture System
EPA	Eicosapentaenoic acid	SFA	Saturated fatty acid
EWSFC	EW Shell Fisheries Center	SMI	Spermarogenic Maturity Index
FAME	Fatty acid methyl esters	VCL	Curvilinear velocity
GoM	Gulf of Mexico		

Chapter 1

Salinity impacts gamete quality in Eastern oyster, *Crassostrea virginica*
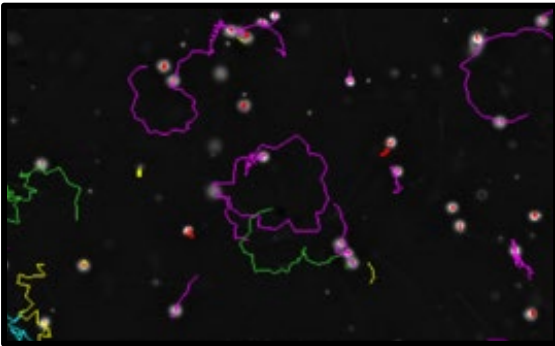
V. MacKenzie Tackett., Helen R. Montague., Jim A. Stoeckel., F. Scott Rikard., Andrea M. Tarnecki., Ian A.E. Butts. Salinity impacts gamete quality in Eastern oyster, *Crassostrea virginica*. Submitted to *Aquaculture* in September 2023

1.1 Abstract

The demands on aquaculture for high-value products, like the Eastern oyster (*Crassostrea virginica*), continue to rise. To aid commercial production, hatcheries mate diploid females with tetraploid males to produce triploid offspring, which in many instances exhibit faster growth than diploid oysters and maintain meat quality during the reproductive season. Many factors limit triploid production by hatcheries, including low gamete quality. While it is known that abiotic factors can influence gamete performance in Eastern oyster, the effects of salinity on triploid production are not well understood. To investigate these effects on gametogenesis and gamete quality, adult tetraploids and diploids were held in recirculating aquaculture systems (RAS) at 10, 20, and 30 PSU for 30 days. Each treatment contained six 140 L tanks with 15 oysters per ploidy. All morphometric measurements were recorded, and the genotypic sex of the oysters determined. Sperm density was quantified from tetraploid males. Sperm motility and velocity were analyzed by Computer Assisted Sperm Analysis, while their viability was determined using flow cytometry. ATP and lipid peroxidation were quantified for tetraploid sperm via bioluminescence and fluorescence, respectively. Eggs from diploid females were assessed for fecundity and size. For tetraploid males and diploid females, lipids from gonadal tissues were analyzed by gas chromatography. Results demonstrated that survival, shell morphometrics, and sperm density were unaffected by salinity. However, variability in sperm density increased when tetraploids were held at 10 PSU. In general, sperm motion was suppressed for oysters held at 10 PSU, relative to the other treatments. Sperm membrane viability was lowest and variability highest in oysters held at 30 PSU. Salinity was not shown to affect the quantity of ATP in sperm. Lipid peroxidation was higher in oysters held at 30 PSU compared to 10 PSU, while those at 20 PSU demonstrated no significant difference compared to other treatments. Variation in lipid peroxidation was highest at

10 PSU. Oocyte irregularities were more prevalent when diploids were held at 10 and 30 PSU. Developmentally crucial lipids, eicosapentaenoic acid (EPA) and docosahexaenoic acid (DHA), from females were highest when oysters were held at 10 PSU, compared to 30 PSU, while neither salinity was statistically different from 20 PSU. Fatty acid concentrations within the sperm from tetraploid males did not differ between salinities. In conclusion, gametes collected from both ploidies held at 20 PSU, performed as well or better than those from the other salinities for every hatchery and gamete-quality metric measured.

1.2 Introduction

Historically, naturally occurring oyster reefs, known for their reliable fisheries harvests, could be found on almost every coast of North America (MacKenzie et al., 1997). From the 1800s into the early 1900s, these reefs were used to collect young, settled oysters, known as spat, while mature adult oysters were harvested for consumption (Manley et al., 2008; Monteforte and Garcia-Gasca, 1994) Over the past fifteen years, overharvesting and climate change have drastically reduced natural populations (Kennedy, 1996; Beck et al., 2011; Moore et al., 2020; Murawski et al., 2021). In Alabama alone, the average harvest was ~850,000 pounds per year prior to 2008, dropping to just over 70,000 that year (NOAA, 2023). Wild harvest regulation changes have the industry on a rebound, with over 283,000 pounds harvested in 2022, but it is still far from a full recovery. This significant reduction in natural populations has encouraged a shift in the Gulf of Mexico (GoM) to aquaculture production, where farms have adapted to using hatchery produced oyster seed. In recent years popularity and demand for cultured oysters has reached historic levels (National Marine Fisheries Service, 2022). In 2019, oyster aquaculture contributed over half of the total 430 million USD produced by all marine aquaculture species (National Marine Fisheries Service, 2022). States bordering the GoM produce the most shellfish by volume compared to other coasts (National Marine Fisheries Service, 2022). In 2019, Mississippi reported 24 farms encompassing 51 acres with 2.8 million oyster seed being cultured (Posadas, 2022). Alabama boasted a farmgate value of 3.2 million USD in 2022 for commercial oyster operations (Grice and Tarnecki, 2023). Additionally, Alabama is now home to at least 15 oyster farms according to Alabama Oyster Aquaculture (2023). Recent funding and legislative changes in Texas, Louisiana, Mississippi, and Alabama have allowed establishment of new oyster facilities to meet growing demands and solidify the economic value of oysters within the region (Walton and Swann, 2021).

The Eastern oyster (*Crassostrea virginica*) is the primary oyster species cultured in the GoM. It is also a keystone species and a vital economic and ecological resource for GoM estuaries (Coen et al., 2007; La Peyre et al., 2013, NOAA, 2022). Like most organisms, Eastern oysters naturally occur as diploids (2n) possessing two sets of chromosomes. However, as commercial demand has continued to rise, ploidy manipulation has been implemented to maximize profits (Stanley et al., 1981). During early embryonic development, chromosomal pairs are induced to be retained which results in polyploidy (Piferrer et al., 2009). Several forms of polyploidy exist including triploid (3n) organisms, which possess one additional set of chromosomes, and tetraploid (4n) organisms which contain two additional pairs. The benefits of triploid oysters are two-fold. Firstly, meat quality remains more consistent in triploid oysters in summer spawning months (Yang et al., 2018). Triploidy inhibits gametogenesis, causing the oysters to spawn infrequently (Nell, 2002; Guo et al., 2009) This lack of spawning maintains meat quality in triploids year-round as compared to their diploid counterparts. Secondly, triploid oysters reach market size faster as less energy is dedicated to reproduction (Bruce and Mann, 1991). These benefits make triploids highly appealing for oyster farming. To induce polyploidy, early-stage embryos are exposed to heat and chemicals; however, there is generally high mortality and variability in success with these methods (Guo et al., 2009). A more reliable method is to produce biological triploids (Guo et al., 1996) by mating tetraploid male and diploid female gametes to create 100% triploid offspring (Guo et al., 1996; Yang et al., 2018).

Previous research suggests that Eastern oyster exposed to extreme low salinity (<6 ppt) in natural habitats have delayed and decreased gametogenesis compared to their high salinity counterparts (Butler, 1949). Additionally, vital functions like filtration, a key factor in building gonadal tissue, are negatively impacted by low salinity (Lavaud et al., 2017). As external broadcast

spawners, it is important for Eastern oyster gametes to be healthy upon release. Sperm health, defined as its ability to fertilize and produce a viable embryo, is largely impacted by environmental conditions (Bobe and Labbé, 2009). Thus, identifying key aspects of health for both male and female gametes can provide insights into fertilization dynamics.

Sperm motility is initiated after introduction into the water column with limited time to reach a viable oocyte (Rurangwa et al., 2004; Song et al., 2009). Swimming kinetics, such as motility and velocity (Boulais et al., 2019; Nichols et al., 2021), are indicative of sperm quality and are typically quantified using computer assisted sperm analysis (CASA) software (Rurangwa et al., 2001; Cosson et al., 2008). When exposed to extreme low (<5 PSU) and high (>30 PSU) salinity, Eastern oyster sperm velocity and motility were significantly impaired, which may ultimately indicate low fertilization success (Dong et al., 2002; Nichols et al., 2021). Pacific oyster (*C. gigas*) also exhibited decreased motility at low salinity (Boulais et al., 2018). Portuguese oyster (*C. angulate*) sperm expressed severe cellular damage at low salinities, which subsequently decreased fertilization rates (JunPeng et al., 2018).

While sperm quality is easily quantifiable, there are few commonly used predictive markers for oyster oocytes. Generally, studies have focused on fertilization success which has shown to be hindered by specific salinity levels (McFarland et al., 2022). While not readily agreed upon, oocyte size and shape have been used to as metric to determine oocyte quality (Boulais et al., 2017). Additionally, lipids contained in oocytes are shown to positively impact embryonic and early-stage larval survival in Eastern oyster (Gallager and Mann, 1986; Gobler and Talmage, 2014). Gallager and Mann (1986) highlighted the relationship between broodstock diet and the accumulation of lipids within oocytes, as it has also been shown that salinity can induce valve closure and reduce filtration lipid accumulation (Pourmozaffar et al., 2020). More recent studies have shown that

increased in steryl esters accumulated within oocytes are detrimental to larval survival (Boulais et al., 2017) adding to the importance of lipid quantification in oocytes as a health metric.

Additionally, hatcheries producing spat are facing threats of climate change as broodstock conditioning in estuaries are reliant on natural conditions. Current climate trends, like increasing temperature and extreme weather events, are predicted to worsen in the next 50 years (IPCC, 2023). Most ecosystems are expected to change, especially those in vulnerable areas like estuaries. Within the southeastern United States there has already been an increase in precipitation events, where intensity of events has increased on the gulf coast (Brown et al., 2019). Coupled with an increase in river discharge and precipitation events, salinity fluctuations and extremes may become more common in the estuaries of the GoM (Prein et al., 2017; Perales-Valdivia et al., 2018). Although temperature and food availability are commonly known to affect gametogenesis in oysters (Shpigel et al., 1992; Boulais et al., 2017; Sühnel et al., 2023), limited information is available on how these salinity changes impact broodstock gametogenesis and the quality of gametes produced. Thus, to fully optimize sustainability and hatchery production, understanding the impacts of salinity on gametogenesis and gamete quality is of the utmost importance.

The primary goal of this study was to examine the effects of salinity (10, 20, and 30 PSU) on gamete production and quality of diploid and tetraploid broodstock. As salinity impacts on reproductive physiology of both tetraploid and diploid oysters have not been fully explored, providing this information for commercial triploid production can aid in increasing larval yield. We hypothesized that low salinity would have the greatest negative impacts on gamete health in male tetraploid and female diploid oysters held in broodstock conditioning systems to produce triploid spat.

1.3 Materials and methods

1.3.1 Oyster culture and maintenance

Diploid (spawned 7/7/2020) and tetraploid (spawned 6/3/2020) oysters were collected on 14 March 2022, from Grand Bay AL (30.3749090ºN, -88.3145984ºW), and transported to the Auburn University Shellfish Lab (AUSL) on Dauphin Island, where they were scrubbed to remove biofouling. Oysters were then separated by ploidy into two 140 L coolers (Igloo brand; Igloo Products Corp., Katy, Texas, USA) and transported to the Aquatic Reproductive Physiology Laboratory (ARPL) at Auburn University, Auburn, AL (32.6526ºN, -85.4859ºW) on 15 March 2022. During transport oysters were housed at 14°C in damp burlap atop chill packs. Upon arrival, tetraploid and diploid oysters were marked with pink or blue nail polish, respectively.

Oysters were initially housed in a recirculating aquaculture system (RAS) at the EW Shell Fisheries Center (EWSFC) in the North Auburn Aquatic Resource Administration Building. The RAS consisted of three 794 L polyethylene round open top tanks (diameter 122 cm × height 81 cm) (Dura-Cast Products, Inc., Lake Wales, FL), seventeen 75 L aquaria (60 cm × 30 cm × 32 cm), two 190 L sump tanks, a heat-pump (AquaLogic Delta Star DSHP-9, Aqua Logic Inc, San Diego, CA, USA), and a UV light sterilizer (Emperor Smart DC2305, Pentair Aquatic Eco-Systems, Apopka, FL, USA). Oysters were randomly placed in each of the three polyethylene round open top tanks (n = 200 per tank). Each day, the oysters were fed ~50 mL of LPB™ Frozen Shellfish Diet to maintain a background algae density between 100,000 and 150,000 cells per mL (Reed Mariculture Inc., CA, USA). Seawater was made by mixing Crystal Sea Marinemix (Marine Enterprises International, LLC, Baltimore, MD) with tap water (originating from deep well aquifers and springs via the City of Auburn, AL) filtered through a reverse osmosis deionization

system (Octopus RO/DI 100 GPD, AquaFX, Winter Park, Florida, USA) to reach a salinity of 20 PSU. The water temperature was maintained at 14 ± 1°C, and photoperiod at 12h L: 12h D.

After 4 days, all oysters transferred to the EWSFC Aquatic Research Center Laboratory where the experimental trial took place. Three RAS within the same room were utilized for the trial. Each RAS was comprised of six 140 L blue cylindrical open top tanks (diameter 58.4 cm × height 53.3 cm), a ⅓ or ½ hp heating/chilling pump (AquaLogic Delta Star DSHP-4 or DSHP-6, Aqua Logic Inc, San Diego, CA, USA), a 430 L bio-tower (diameter 35 cm × height 122 cm), a UV light sterilizer (Aqua Ultraviolet Classic UV 57 Watt Series, Aqua Ultraviolet, Temecula, CA, USA), a 415 L polyethylene sump (67 cm × 70.5 cm × 88 cm), a 1 hp submersible pump (Pond-MAG 1800, Danner Manufacturing, Inc., Islandia, NY, USA), and a temperature/flow rate monitoring system (Sensaphone Sentinel, Sensaphone, Aston, PA, USA). Each cylindrical tank was equipped with a 16-gauge mesh stand to elevate oysters ~15 cm from the bottom of the tank. Tanks also had diffused air and upwelling water at a flow rate of ~6 L/min. Artificial seawater was prepared as previously described to achieve desired salinities. Oysters (n = 15 per ploidy) were acclimated to experimental RAS systems over a 14-day period before salinity treatments were initiated. During acclimation, water temperature was maintained at 16.0 ± 0.5°C, salinity at 20 ± 1 PSU, and photoperiod at 12h L: 12h D.

1.3.2 Experimental design

After the 14-day acclimation period, salinity was slowly adjusted (< 3 PSU per day) in each RAS to the desired salinity treatment (10, 20, or 30 ± 2 PSU). Treatment salinities were then maintained for 30 days. Water temperature and photoperiod were adjusted weekly to mimic natural conditions based on average values for the previous week in the GoM (range = 16-19°C; 12h L: 12h D to 13h L: 11h D at 75 ± 5 lux). Temperature and salinity were monitored daily using a YSI

55 multiparameter instrument (model 58 with 550A probe; YSI, OH, USA) and refractometer (Vee Gee STX-3, Vee Gee Scientific, IL, USA), while nitrite, nitrate, pH, hardness, and alkalinity were measured daily using a water quality test kit (All-purpose 5-way test strips, Lifeguard Aquatics, CA, USA). Total ammonia nitrogen (TAN) was measured with a spectrophotometer (D/R 2000 Direct Reading, Hach, Colorado, USA). Mean nitrite levels in the three RAS ranged from 1.61 to 2.06 mg/L, TAN from 0.15 to 0.18 mg/L, pH from 6.95 to 6.98, alkalinity 78.75 to 79.38 mg/L CaCO$_3$, and hardness 240.00 to 241.88 mg/L. Oysters in each RAS were fed LPB™ Frozen Shellfish Diet (Reed Mariculture Inc., CA, USA) three times daily (08:00, 12:00, 16:00), either by hand or automatic GHL doser (GHL doser 2.1, Rheinland-Pfalz Deutschland, Germany). Feeding quantity increased per day from 50 mL to 150 mL in each RAS to maintain desired background algae as the trial progressed. All tanks were monitored daily for mortality. Detritus was siphoned from tank bottoms along with a 30 % daily water exchange.

1.3.3 Data collection

Sex determination and morphology

After 30-days all oysters were removed from all tanks for sampling, tanks were sampled at random. A precision standard balance (TS200-02; Ohaus corporation, New Jersey, USA) and digital calipers (VWR, Item number 12777-830, Pennsylvania, USA) were used to measure shell height (± 0.03 mm), shell length (± 0.03 mm), shell width (± 0.03 mm), and whole wet tissue weight (± 0.01 g). Each oyster was opened at the hinge, left valve resting on the table, using a shucking knife. After releasing the hinge, the adductor muscle was severed from the right valve to fully open the oyster. All tools were rinsed in 90% ethanol between individuals. Mantle tissue was thoroughly rinsed of excess salt water with deionized water. The remaining liquid was blotted from

tissue with Kim wipes. Sex was determined using a 1 µL sample of gonad viewed with a Zeiss Axiolab 5 microscope (Carl Zeiss Microscopy, LLC, New York, USA) equipped with 20× objective with negative phase contrast (SAF "A-Plan" 20x/0.45 Ph-n 1). The first 3 tetraploid males and diploid females were utilized for lipid analysis. The following 5 tetraploid males were utilized for sperm cell density, kinematics, viability, ATP, and oxidative stress. Finally, the next 3 diploid females were used to determined fecundity and egg morphology.

1.3.3.1 Tetraploid sperm quality analyses

Cell density

Semen was collected by creating shallow slices in the gonadal tissue with a sterile 20-gauge scalpel while avoiding digestive tissue. Semen was then extracted with 1000 µL pipette tips, transferred to 1.5 µL microcentrifuge tubes, and held at 19°C in an Echotherm™ Chilling/Heating Dry Bath (Torrey Pines Scientific, California, USA) for the duration of the analysis. Immediately following collection, 1 µL of sperm was observed using a Zeiss Axiolab 5 microscope equipped with 20× objective with negative phase contrast to determine if sperm were activated. If actively swimming sperm were present the sample was disposed of, and another individual was utilized. Non-activated sperm were diluted with artificial salt water (ASW; 516 mM NaCl, 10.4 mM KCl, 11 mM $CaCl_2 \times 2H_2O$, 34 mM $MgCl_2 \times 6H_2O$, 22 mM $MgSO_4 \times 7H_2O$; Boulais et al., 2018). Dilutions ranged from 100 to 400× depending on initial densities. Sperm density (cells/mL) was determined for each male, in duplicate, using a Neubauer hemocytometer following Myers et al. (2020). In brief, once sperm were diluted in ASW, samples were homogenized for ~10 s, then 10 µL was pipetted onto the hemocytometer. Sperm settled onto a 5×5 grid (1 mm^2), where sperm

inside five squares (0.2 mm^2; top left, top right, bottom right, bottom left, and center) were counted. To determine the average cell density of the diluted sperm, all counts were summed and multiplied by 5 to estimate the number of sperm cells in the entire grid. The dilution factor was multiplied by the estimated sperm cells in the 5×5 grid and multiplied by 10,000 (to identify cells/ mL).

Swimming kinematics

Sperm activation solution was prepared using 516 mM NaCl, 10.4 mM KCl, 11 mM CaCl$_2$, 34 mM MgCl$_2$, and 22 mM MgSO$_4$ (Nichols et al., 2021) and salinity adjusted from 40 PSU to 20 PSU using ultrapure water (Milli-Q® Advantage A10 Water Purification System, Merck KGaA, Darmstadt, Germany). Pluronic F-127 (0.4%; Sigma Aldrich, Missouri, USA) was added to prevent sperm from sticking to glass slides. Activation solution was buffered to ~7.5 pH with 20 mM Tris. Activation solution (99 to 399 µL) was pipetted into 1.5 mL microcentrifuge tubes and placed into an Echotherm™ Chilling/Heating Dry Bath set to 19°C. To activate sperm motility, roughly 1.0 µL of semen was diluted into prefilled microcentrifuge tubes and rapidly inverted several times to mix thoroughly. Next, 5 µL of activated sperm were immediately pipetted into a 20 µm deep 2X-CEL chamber (Hamilton Thorne Biosciences, Massachusetts, USA), under a light microscope (same as listed in Section 2.3.1.). Motility was recorded in triplicate at 20× magnification at 30, 60, and 120 s post-activation for each male. Sperm motility (%) and curvilinear velocity (VCL; µm/s) were then determined using CASA software (CEROS II, Hamilton Thorne Biosciences, Massachusetts, USA). CASA videos were taken at 60 frame/s, exposure was set to 4 milliseconds, and camera gain at 300. Cells were tracked between 3 to 11 µm, minimum cell brightness was set at 57, and the photometer range of illumination fields were

between 55 and 65. All videos were manually examined to verify accuracy following Butts et al. (2011). If software mistakenly split a single sperm track, combined crossing tracts of multiple sperm, or marked motile sperm as stagnant, tracks were removed from the analysis. Tracks were also removed if sperm were drifting over the field of vision, rather than actively swimming.

Viability

Sperm cell viability was assessed by flow cytometry following proprietary protocols in the Muse® Count and Viability kit (Luminex, Texas, USA). The kit utilizes two fluorescent dyes, in which one is a membrane permeable fluorescent dye that stains all cells with a nucleus and distinguishes cells from debris in the sample. The second fluorescent dye only stains dead or dying cells that have lost membrane integrity, to distinguish dead and dying cells from healthy ones. First, cells were diluted in triplicate with ASW ranging from 1×10^6 to 1×10^7 cells/mL, then 20 µL of cell suspension was mixed with 380 µL of Count and Viability Reagent in 1.7 mL microtubes. The solution was incubated for 5 min in the dark at 21-22°C before being quantified in the Guava Muse Cell Analyzer® (EMD Millipore Corporation, Massachusetts, USA). To ensure cellular debris was excluded the Cell Size Index sliders (gates) were adjusted to only include the living and dead sperm cells. A secondary gate, the viability discriminator, was then adjusted to differentiate viable cells and dead cells.

Adenosine 5'-triphosphate

Adenosine 5′-triphosphate (ATP) was quantified for sperm using an ATP bioluminescence assay kit (FLAA-1KT, Sigma-Aldrich, Munich, Germany). In brief, 5 µL of semen was added to 5 µL of ASW and 495 µL of boiling lysing buffer (25 mM HEPES, 10 mM $Mg(CH_3COO)_2$, 2 mM $C_{10}H_{16}N_2O_8$, 3 mM NaN_3, pH 7.75; Perchec et al., 1995) in 1.5 µL microcentrifuge tubes. All tubes were placed in boiling water (98 - 100°C) for 2 min and centrifuged at 14,000 × g (4°C) for 15 min. Supernatant was removed and stored at -20°C to be used for analysis while the pellet was discarded. Samples were placed in white opaque 96 well plates (LUMITRAC™ 200, 82050-726, VWR, Pennsylvania, USA) with appropriate reagents and luminescence was immediately read using a multifunctional microplate reader (Cytation 3, Biotek, California, USA). When calculating ATP content, the standard method provided in the kit manual was utilized and the mean of all measurements per male was used for statistical analyses. Final values were reported as nanomoles ATP per 10^9 sperm.

Oxidative stress

Lipid peroxidation was quantified by detecting malondialdehyde (MDA) present in samples using Cayman chemicals TBARS Assay Kit (No. 10009055, Michigan, USA). In brief, 25 mg (± 0.01 mg) of gonadal tissue was homogenized with 250 µL RIPA Buffer containing protease inhibitor cocktail. Samples were loaded in a 4-Place Mini Bead Mill Homogenizer (10158-558, VWR) at level four for 30 s. Tubes were then centrifuged at 1,600 × g for 10 min (4°C) and the supernatant was stored at -20°C for further analysis. When performing the final analysis, the

supernatant was returned to 4°C and added to 10 mL centrifuge tubes with appropriate reagents according to the manual provided and placed in boiling water (98 - 100°C) for 60 min. After removing from boiling water all tubes were incubated on ice for 10 min and centrifuged for 10 min at 1,600 × g (4°C). Supernatant was pipetted into black 96-well plates provided in the kit and immediately read at excitation wavelength 530 nm and emission wavelength 550 nm using a Synergy HTX multi-mode reader (Synergy HTX multi-mode reader, Biotek, California, USA). MDA concentrations were determined using the standard method provided and reported in nanomoles MDA per 1 mL gonad homogenate. The mean of all measurements per male was used for statistical analyses.

1.3.3.2 Maternal analyses

Oocyte collection and quantification

After identifying female oysters, all tissue from a given diploid female was collected and placed in 300 mL of 20 PSU saltwater prepared with ultra-pure water and Crystal Sea Marinemix. The tissue was macerated, using a scalpel, until the tissue was fully homogenized to release oocytes from gonadal tissue. To separate large tissue debris, the homogenized mixture was sieved through a 100 μm screen. The suspension was left to rest for 10 min to normalize before mixing to resuspend oocytes. To quantify oocytes, 1 mL of the homogenized oocyte mixture was pipetted into a VWR Sedgwick Rafter counting chamber (VWR, Item Number 66197-008). After 5 min of settling the oocytes were quantified using a Zeiss Imager.A2 (Carl Zeiss Microscopy, LLC) with 10× Plan Achromat phase contrast objective (A-Plan 10 ×/ 0, 25 Ph 1-, Carl Zeiss Microscopy, LLC). For this analysis, 30 random cells were counted in duplicate for each female. To determine

total egg density an average of both counts was multiplied by the volume (1000 mm^3) then divided by the total counting area (50 mm × 20 mm × 1 mm) and number of transects counted (n = 30).

Oocyte morphology

Three diploid females were sampled from each tank at the end of the trial. Then digital images of a minimum of 12 oocytes per female were collected to analyze morphometrics (3 females × 5 tanks × 12 oocytes = 180 oocytes per salinity treatment). Strip-spawned oocytes were allowed to rest for a 20 min normalizing period. After resting, the oocyte suspension was homogenized and digital images were taken using a light microscope (Zeiss Imager.A2, listed above) and Axiocam 305 camera (Carl Zeiss Microscopy, LLC) with Zen Pro imaging software (v. 6.1).

Length (longest measurement from one edge of membrane through yolk to other edge of membrane), and width (widest point from one edge of membrane through yolk to other edge of membrane) were acquired for each oocyte using the "Analyze" function of ImageJ (Fig. 1.8A, Schneider et al., 2012). Additionally, irregularities were identified and quantified. In brief, if an oocyte's yolk was touching the edge of the membrane or protruding through the membrane, the oocyte was considered irregular (Fig. 1.8A). Percent of irregularities per female were quantified as the total number of irregular eggs divided by the total number of eggs measured and multiplied by 100.

Lipid quantification

Samples of gonadal tissue (~100 mg) were taken in duplicate from each oyster, placed in 1.5 μL microcentrifuge tubes, and immediately stored at -20°C until being shipped to The University of Texas at Austin in a Styrofoam cooler with dry ice. Upon arrival, samples were held in a -20°C

freezer. Fatty acids and total lipids were determined using gas chromatography following Faulk and Holt (2005). In brief, all tetraploid male oysters (n = 5) sampled from each tank were pooled before lipid extraction. Diploid females (n = 3) were pooled in the same fashion. Total lipids were cold extracted from lyophilized samples with chloroform/methanol (2:1, v/v) following Folch et al. (1957). Butylated hydroxytoluene (0.01%, w/v) was added as an antioxidant. Crude lipid extracts from oyster gonadal tissues were measured gravimetrically, following evaporation of the solvent using nitrogen. Total lipids were saponified in 0.5 M KOH and fatty acid methyl esters (FAMEs) were prepared by transesterification with 14% boron trifluoride in methanol following Morrison and Smith (1964). FAMEs were analyzed on a Hewlett-Packard 5890A gas chromatograph equipped with a flame ionization detector and a Supelcowax 10 fused silica capillary column (30 mm long, 0.53 mm internal diameter, 1.0 µL thickness; Supelco, Inc., Pennsylvania, USA). FAME peaks were recorded using Tigre II analog/digital interface and Chrom Perfect Spirit software (Justice Laboratory Software, Palo Alto, California, USA). Individual peaks were identified by comparison to chromatograms of known standards (Supelco, Inc., Pennsylvania, USA).

1.3.4 Statistical analyses

All data were analyzed using SAS statistical analysis software (v. 9.1; SAS Institute Inc., Cary, NC, USA). Residuals were tested for normality (Shapiro–Wilk test) and homogeneity of variance (plot of residuals vs. predicted values). When necessary, data were $\log_{10}$ transformed or arcsine square-root transformed (percentage data) to meet assumptions of normality and homoscedasticity. The Kenward–Roger procedure was used to approximate denominator degrees of freedom for all F-tests (Spilke et al., 2005). Error bars represent least square means standard error. To examine the effect of salinity and time post-activation on sperm kinematic traits, data were analyzed using a

series of repeated measures factorial ANOVA models. Each model contained salinity and post-activation time, as well as the corresponding salinity × post-activation time interaction. In the case of a significant interaction, the models were broken down into individual one-way ANOVA models at each post-activation time. These revised models involved only preplanned comparisons and did not include repeated use of the same data, so alpha-level corrections for posteriori comparisons were not necessary. If a nonsignificant interaction was detected the main effects of salinity and time were interpreted. Mixed-model ANOVA was used for survival, shell morphology, sperm density, membrane viability, ATP concentration, oxidative stress, lipid quantities, egg fecundity, and egg morphology to determine difference among salinity treatments. Treatment means were contrasted using the Tukey's test. Alpha was set at 0.05 for main effects and interactions.

The coefficient of variation ($CV = \frac{\text{Standard deviation}}{\text{Sample mean}} \times 100$) was determined for survival, shell morphology, sperm density, sperm kinematics, membrane viability, ATP concentration, oxidative stress, egg fecundity, and egg morphology. A series of one-way ANOVA models were used to examine the degree of variability between salinity treatments.

1.4 Results

After the experimental trial ended, mean (± SEM) tetraploid survival ranged from 85.6% ± 3.8 at 10 PSU to 94.4% ± 3.5 at 30 PSU. Survival for diploids ranged from 87.8% ± 2.1 at 10 PSU to 95.6% ± 2.1 at 20 PSU. Differences in survival among salinities were not statistically significant for either ploidy ($F_{2,12} \leq 3.71$, $P \geq 0.056$; Fig. 1.1A-B).

Mean diploid shell length, width, and height ranged from 56.5 to 58.8 mm, 29.4 to 30.0 mm, and 80.7 to 84.0 mm, respectively. The same measurements for tetraploids ranged from 61.2 to 64.4 mm, 33.8 to 34.8 mm, and 104.5 to 109.2 mm, respectively. All shell morphometric

measurements for both diploids ($F_{2,12} \leq 1.96$, $P \geq 0.183$) and tetraploids ($F_{2,12} \leq 2.26$, $P \geq 0.147$) were not significantly different between salinity treatments. Furthermore, variation between replicates was not significantly different for shell morphometric measurements in diploids ($F_{2,12} \leq 2.57$, $P \geq 0.117$) or tetraploids ($F_{2,12} \leq 1.14$, $P \geq 0.352$).

1.4.1 Reproductive performance in tetraploid males

Sperm density

Sperm density tended to increase when the tetraploids were held at higher salinities, however there were no significant differences in sperm density among any of the salinity treatments ($F_{2,12}$ = 1.76, P = 0.214; Fig. 2A). Male-to-male variation in sperm density was significantly higher when the tetraploids were held at 10 PSU ($F_{2,12}$ = 6.70, P = 0.011; Fig.1.2B).

Computer Assisted Sperm Analyses (CASA) and viability

Sperm were motile across the entire salinity gradient (Fig. 1.3A). The salinity × time post-activation interaction was significant for sperm VCL ($F_{4,24}$ = 6.59, P = 0.001). Therefore, the effects of salinity were analyzed at each time post-activation. At 30 s ($F_{2,12}$ = 12.82, P = 0.001; Fig. 1.3B) and 60 s post-activation ($F_{2,12}$ = 6.53, P = 0.012; Fig. 1.3B) oysters held at 10 PSU had lower VCL compared to those held at 20 PSU. However, at 120 s post-activation ($F_{2,12}$ = 0.29, P = 0.757; Fig. 1.3B) holding salinity did not impact sperm VCL.

The interaction between the main factors (salinity × time post-activation) was also significant for sperm motility ($F_{4,24}$ = 3.73, P = 0.017). Therefore, the effects of salinity treatment and time post-activation were interpreted. There was an impact of holding salinity, where sperm motility

was suppressed at 30, 60, and 120 s post activation when oysters were held at 10 PSU ($F_{2,12} \geq 6.9$, $P \leq 0.010$; Fig. 1.3C).

Once again, the interaction between the main factors (salinity × time post-activation) was significant for progressive VCL ($F_{4,24} = 6.03$, $P = 0.002$); thus, main effects were interpreted. Oysters conditioned at 10 PSU had significantly lower progressive VCL at 30 to 120 s post-activation ($F_{2,12} \geq 18.18$, $P \leq 0.0002$; Fig. 1.3D). CASA analyses showed no interaction between the main factors (salinity × time post-activation) for progressive motility ($F_{4,24} = 0.79$, $P = 0.545$; Fig. 1.3E). Sperm kinematics were shown to be suppressed for oysters held at 10 and 30 PSU relative to 20 PSU, with the largest effects seen at 10 PSU, when the main effects of salinity were considered ($F_{2,24} = 103.21$; $P < 0.0001$; Fig. 1.3F). Time post-activation did not affect progressive motility ($F_{2,12} = 1.16$; $P = 0.331$; Fig. 1.3F).

Male-to-male variation within treatments was also examined for all sperm kinematics. Salinity × time post-activation interactions were not significant for VCL ($F_{4,24} = 0.21$, $P = 0.928$; Fig. 1.4A-B), motility ($F_{4,24} = 2.39$, $P = 0.079$; Fig. 1.4C-D) or progressive motility ($F_{4,24} = 1.25$, $P = 0.315$; Fig. 1.4G-H). The main factors were only significant for progressive VCL ($F_{4,22.2} = 2.95$, $P = 0.043$; Fig. 1.4E). Here, variation increased when oysters were held at 10 PSU, at each time post-activation, indicating less consistent progressive velocity among males examined.

Salinity of holding water affected sperm viability with the highest mean values reported at 10 and 20 PSU, and the lowest values reported at 30 PSU ($F_{2,12} = 14.03$, $P = 0.0007$; Fig. 1.5B). Additionally, male-to-male for sperm viability was higher when males were held at 30 PSU compared to the other salinity groups ($F_{2,12} = 14.53$, $P = 0.001$; Fig. 1.5C).

Adenosine 5'-triphosphate

Holding salinity did not significantly impact ATP concentration for tetraploid males ($F_{2,12}$ = 1.01, P = 0.393; Fig. 1.6A). Additionally, male-to-male variation in ATP was not significantly different across the salinity groups ($F_{2,12}$ = 0.07, P = 0.933; Fig. 1.6B).

Oxidative stress

When examining MDA levels in tetraploid males, concentrations were higher in oysters held at 30 PSU than those held at 10 PSU, while 20 PSU was not statistically different from either ($F_{2,12}$ = 3.88, P = 0.050; Fig. 1.6C) and male-to-male variation was highest in oysters held at 10 PSU ($F_{2,12}$ = 11.73 P = 0.002; Fig. 1.6D).

1.4.2 Reproductive performance in diploid females

Egg fecundity

There was no significant difference in fecundity of diploids among salinity treatments ($F_{2,12}$ = 0.01, P = 0.993; Fig. 1.7A). In addition, female-to-female variation in fecundity did not differ significantly within salinity treatments ($F_{2,12}$ = 1.17, P = 0.344; Fig. 1.7B).

Egg morphometrics

Egg length and width did not differ significantly with salinity ($F_{2,12} \leq 0.77$, $P \geq 0.484$; Fig. 1.7C-E) nor did variation for either measurement among salinity treatments ($F_{2,12} \leq 0.26$, $P \geq 0.774$; Fig. 1.7D-F). Significantly more egg irregularities were observed when females were held at 30 PSU ($F_{2,12} = 22.77$, $P < 0.0001$; Fig. 1.8B), while female-to-female variation in irregularities within treatment groups did not differ significantly with salinity ($F_{2,12} = 0.31$, $P = 0.740$; Fig. 1.8C).

1.4.3 Lipid quantification

Fatty acid concentrations within tetraploid male gonad tissue did not differ between salinity treatments (Table 1.1). However, most lipids tended to decrease as the salinity increased. The concentration of several saturated fatty acids (SFA) in diploid female's gonad tissue were significantly higher at 10 PSU compared to 30 PSU, however neither were statistically different form 20 PSU (Table 1.2). Specifically, 15:0, 16:0, 22:6n3 (docosahexaenoic acid; DHA) were all higher when females were maintained at 10 PSU compared to females at 30 PSU. Furthermore, polyunsaturated fatty acids (PUFA) followed a similar trend, where 18:2n6, 18:3n6, 18:3n3, 20:4n6, 20:5n3 (eicosapentaenoic acid; EPA), and 22:5n3 were significantly higher for females held at 10 PSU compared to 30 PSU. Total monounsaturated fatty acids (MUFA) did not differ between salinity groups, however, specific MUFA like 16:2n4, 18:1n9, and 20:1n9 were all significantly higher for females held at 10 PSU compared to those at 30 PSU.

1.5 Discussion

Although variability in abiotic factors such as pH (Boulais et al., 2017; Clements et al., 2021), temperature (Rodríguez-Jaramillo et al., 2022), and salinity (Gregory et al., 2023; Mcfarland et al.,

2013) are known to impact oysters, most research has focused on the cellular and physiological effects of stress on larval, juvenile, and adult Eastern oyster. Conversely, very little is known about how abiotic stressors, specifically salinity, impact oyster gametogenesis at cellular and molecular levels or how these stressors impact the phenotype and epigenome of adults and their ensuing gametes and offspring. Insight into the effects of salinity on gamete health of tetraploid and diploid broodstock is of critical importance to meet the increasing demand for hatchery production of triploid oysters.

As metabolic pathways and oyster physiology are heavily reliant on one another, negative impacts of salinity are an important factor when housing broodstock (Pourmozaffar et al., 2020). Valve closure due to salinity extremes (<10 PSU) or salinity fluctuations have been shown to decrease filtration and reduce food intake in Eastern oyster (Fuhrmann et al., 2016; Mcfarland et al., 2013). Persistent valve closure can lead to decreases in growth rates and, in more extreme cases, exhaustion of energetic reserves which results in death (Kooijman, 2009; Pourmozaffar et al., 2020). This study aimed to produce healthy gametes; thus, salinity treatments were above and below thresholds known to cause excessive mortality in Eastern oyster. Here, survival was above 85% in all salinity treatments; additionally, survival among treatments was not significantly different. Furthermore, growth was not negatively impacted in any salinity treatment nor was it significantly different among treatments. Indicating the salinity levels studied did not negatively affect the filtration or survival of the study oysters.

Many of the previous studies examining the relationship between salinity and gamete development have shown gametes develop slower in low salinity environments (Butler, 1949; Shumway, 1996; La Peyre et al., 2013), however in this study, there was no significant impact of salinity on mean sperm counts. These conflicting results are likely due to the nature of the

experimental set-ups. Unlike the aforementioned studies which investigated salinity impacts in estuarian environments, the current study was performed in a controlled lab setting. These previous studies also focused on short term exposure to varying salinities, with much wider salinity ranges, as low as 3 PSU or as high as 30 PSU. In contrast to this, more recent studies like Gregory et al. (2023) found that low salinity encouraged gametes earlier in the spawning season and gametes were produced for a longer period over the season in these same individuals. This was noted to be due to genetic plasticity of the broodstock. Salinity tolerance is now being connected to heritable traits in Eastern oyster, where results suggest that specific breeding may select for oysters with a lower salinity tolerance (McCarty et al., 2020). As their research has shown expanded salinity tolerance, oysters may be able to dedicate more energy to reproduction rather than maintaining normal functions because of the chosen breeding lines in lower salinity areas. While the family lines of oysters used in this study were not chosen because of salinity tolerance, these lines may be more tolerant than others as sperm density was unaffected by salinity in this study. Ultimately, more research is needed to fully understand how genetics could potentially play a role with gamete development in varying salinity environments.

Sperm motility and velocity were quantified as they are directly linked to fertility in bivalves (Boulais et al., 2019; Dong et al., 2002). Here, the percent of motile sperm decreased in tetraploid males held at 10 PSU. Additionally, these cells had decreased VCL during the first 60 s post activation. Conversely, sperm membrane viability was negatively impacted by the high salinity treatment. ATP powers sperm locomotion and can be used as an indicator of fertilization success as well as potentially indicating membrane integrity (Boulais et al., 2017). We found there was no significant difference among salinity treatment groups or variation within groups. Additional energetic testing such as mitochondrial respiration may be able to shed light on sperm kinematic

behaviors. As oyster sperm swims for extended periods of time, continuous synthesis of ATP is needed to power flagellar motion (Boulais et al., 2019). As a result, mitochondrial respiration is closely linked to the activation of sperm motility and can be used to determine how the electron transport chain is being influenced during swimming (Boulais et al., 2019). By analyzing this metabolic pathway, it may reveal how other mechanisms are responsible for flagellar movement in the first 2 h of active swimming, similar to results found in *C. gigas* (Boulais et al., 2019). Furthermore, findings by Boulais et al. (2017) suggest that a positive correlation between motility and velocity can indicate that swimming velocity may be influenced by maturation occurring during spermatogenesis. As new sperm cells are continually produced in oysters, strip spawning would collect both mature sperm as well as spermatogonia (Franco et al., 2008). This may indicate that broodstock in 10 PSU holding tanks had inhibited sperm maturation when compared to those in the 20 or 30 PSU. This would be supported by previous findings, where low salinity inhibited sperm maturation and delayed spawning in oysters (Butler, 1949; Shumway, 1996; La Peyre et al., 2013). A continuation of the same study by Boulais et al. (2017) found positive relationships between ATP concentrations and sperm membrane viability. In our study, ATP was not significantly different, indicating other intracellular regulatory mechanisms may be more influential than previously thought. Ultimately, further research is needed in this area to better understand this relationship.

Environmental stress can also be detected using oxidative stress levels, as under suboptimal conditions MDA levels increased in oysters (Alves de Almeida et al., 2007; Zanette et al., 2011; Sadri and Khoei, 2023). Oxidative stress has also been shown to increase during gamete production in oysters as more metabolic energy is devoted to the generation of gametes (Béguel et al., 2012). However, if the rate of reactive oxygen species (ROS) production exceeds what an organism can

accommodate with its own defense mechanisms, the oxidation of lipids, proteins, and DNA occurs (Sies, 1993). Elevated MDA levels of broodstock have been shown to increase the number of deformities when larvae reach D stage (pre-set) (Mai et al., 2014). We saw an increase in oxidative stress in male tetraploids held at 30 PSU compared to those held at 10 PSU. To determine if the oxidative stress reached levels which would impact lipids within the gonad tissue, fatty acid compositions were then examined.

Lipid content in gonadal tissue is used as an indicator of gamete quality (Dridi et al., 2006), fertility (Boulais et al., 2015), and gonadal development (Subasinghe et al., 2019) in oysters. As previously mentioned, lipids are exceptionally vulnerable to oxidative stress due to the unsaturated polysaccharides (Barrera, 2012). Here, it was anticipated that because elevated MDA levels were observed in 30 PSU males, there would also be a significant difference in lipid content. While there was no significant difference in tetraploid male lipids, total PUFA, MUFA, and SFA were highest at 10 PSU and declined as the salinity increased. Previous studies have shown low salinity levels can decrease lipid content within oyster, likely due to a higher metabolic cost and reduced filtration (Pourmozaffar et al., 2020). Accumulation of lipids is driven by broostock diet whose uptake is linked to filtration; therefore, decreased filtration in oysters held in poor environmental will hinder lipid accumulation (Soudant et al., 1996a; Soudant et al., 1996b). However, an acclimation period to altered salinity levels has been shown to offset these effects depending on oyster lineage (Pourmozaffar et al., 2020). Conversely, in diploid females, specific lipids did decrease significantly as the salinity increased. Total PUFAs and SFAs decreased between females held at 10 PSU and 30 PSU. Of total PUFAs and SFAs that decreased two of the most notable were 20:5n3 (EPA) and 22:6n3 (DHA). In bivalves, omega 3 fatty acids such as DHA play a critical role in embryonic development, where studies have shown that environmental factors can inhibit the

34

accumulation of this lipid (Whyte et al., 1990, 1991; Glandon et al., 2016). Additionally, elevated DHA and EPA levels can indicate healthy oocytes as well as the potential for higher larval survival (Glandon et al., 2016).

More irregular oocytes were observed when oysters were held at 10 or 30 PSU. However, no differences were seen in the quantity of oocytes produced between salinity groups. Oocyte size and shape have been shown to influence fertilization success in marine fishes and are speculated to affect oysters as well (Baynes and Howell, 1996; Sussarellu et al., 2016). As oocytes tend to homogenize in size and shape toward the end of the maturation, strip spawning sampled all developing oocytes (Lango-Reynoso et al., 2000). Both round and pear-shaped oocytes are common in oysters, however pear shapes are generally corrected if the oocytes hydrate in a saltwater solution before fertilization (Thanormjit et al., 2020). Thus, pear shapes were not considered "irregular" in this study. For the current study, additional abnormalities were seen, where oocyte nuclei protruded through the oyster membrane which likely would not be corrected regardless of additional homogenization period. These irregularities could indicate a delay in the development and standardization of the oocytes at 10 and 30 PSU.

1.6 Conclusions

To the best of our knowledge environmental salinities and their impacts on gametogenesis and gamete quality have not yet been investigated in tetraploid and diploid Eastern oyster. This information will not only contribute to the continually expanding aquaculture industry by informing broodstock conditioning and spawning optimization but can also act as a predictor for reproductive output from broodstock held in off-bottom aquaculture gear. Understanding how salinity changes will impact broodstock is vital as estuarine environments continue to be altered by climate change. Overall, these results show that holding salinity does affect the gamete quality

of both tetraploid male and diploid female Eastern oyster. This study highlights the importance of an understudied abiotic factor (salinity) in the reproductive cycle of one of the most valuable bivalves in the Southeastern United States and provides vital information which can be utilized in hatcheries to optimize triploid spat production. The data in this study could also aid in selecting sites to house oysters that are conducive to natural conditioning, ultimately improving access to ripened broodstock to support the growing oyster aquaculture industry.

1.7 References

Alves de Almeida, E., Celso Dias Bainy, A., Paula de Melo Loureiro, A., Regina Martinez, G., Miyamoto, S., Onuki, J., Fujita Barbosa, L., Carrião Machado Garcia, C., Manso Prado, F., Eliza Ronsein, G., Alexandre Sigolo, C., Barbosa Brochini, C., Maria Gracioso Martins, A., Helena Gennari de Medeiros, M., Di Mascio, P., 2007. Oxidative stress in Perna perna and other bivalves as indicators of environmental stress in the Brazilian marine environment: Antioxidants, lipid peroxidation and DNA damage. Comparative Biochemistry and Physiology Part A: Molecular & Integrative Physiology, 146(4), 588–600. https://doi.org/10.1016/j.cbpa.2006.02.040

Barrera, G., 2012. Oxidative stress and lipid peroxidation products in cancer progression and therapy. ISRN Oncology, 2012, 1–21. https://doi.org/10.5402/2012/137289

Baynes, S. M., Howell, B. R., 1996. The influence of egg size and incubation temperature on the condition of Solea solea (L.) larvae at hatching and first feeding. Journal of Experimental Marine Biology and Ecology, 199(1), 59–77. https://doi.org/10.1016/0022-0981(95)00189-1

Beck, M. W., Brumbaugh, R. D., Airoldi, L., Carranza, A., Coen, L. D., Crawford, C., Defeo, O., Edgar, G. J., Hancock, B., Kay, M. C., Lenihan, H. S., Luckenbach, M. W., Toropova, C. L.,

Zhang, G., Guo, X., 2011. Oyster Reefs at Risk and Recommendations for Conservation, Restoration, and Management 61(2), 107–116. https://doi.org/10.1525/BIO.2011.61.2.5

Béguel, J.-P., Huvet, A., Quillien, V., Lambert, C., Fabioux, C., 2012. Study of the antioxidant capacity in gills of the Pacific oyster Crassostrea gigas in link with its reproductive investment. https://doi.org/10.1016/j.cbpc.2012.10.004

Bobe, J., Labbé, C. 2009. Egg and sperm quality in fish. General and Comparative Endocrinology, 165, 535–548. https://doi.org/10.1016/j.ygcen.2009.02.011

Boulais, M., Corporeau, C., Huvet, A., Bernard, I., Quere, C., Quillien, V., Fabioux, C., & Suquet, M., 2014. Assessment of oocyte and trochophore quality in Pacific oyster, Crassostrea gigas. https://doi.org/10.1016/j.aquaculture.2014.11.025

Boulais, M., Demoy-Schneider, M., Alavi, S. M. H., Cosson, J., 2019. Spermatozoa motility in bivalves: Signaling, flagellar beating behavior, and energetics. Theriogenology, 136, 15–27. https://doi.org/10.1016/J.THERIOGENOLOGY.2019.06.025

Boulais, M., Soudant, P., Le Goïc, N., Quéré, C., Boudry, P., Suquet, M., 2015. Involvement of mitochondrial activity and OXPHOS in ATP synthesis during the motility phase of spermatozoa in the pacific oyster, Crassostrea gigas. Biology of Reproduction, 93(5), 1–7. https://doi.org/10.1095/BIOLREPROD.115.128538/2434309

Boulais, M., Soudant, P., Le Goïc, N., Quéré, C., Boudry, P., Suquet, M., 2017. ATP content and viability of spermatozoa drive variability of fertilization success in the Pacific oyster (Crassostrea gigas). https://doi.org/10.1016/j.aquaculture.2017.05.035

Boulais, M., Suquet, M., Arsenault-Pernet, E. J., Malo, F., Queau, I., Pignet, P., Ratiskol, D., Grand, J. Le, Huber, M., Cosson, J., 2018. PH controls spermatozoa motility in the Pacific oyster (Crassostrea gigas). Biology Open, 7(3).

https://doi.org/10.1242/BIO.031427/259283/AM/PH-CONTROLS-SPERMATOZOA-MOTILITY-IN-THE-PACIFIC

Brown, V. M., Keim, B. D., Black, A. W., 2019. Climatology and Trends in Hourly Precipitation for the Southeast United States. Journal of Hydrometeorology, 20(8), 1737–1755. https://doi.org/10.1175/JHM-D-19-0004.1

Bruce, J., Mann, R. L., 1991. Sterile Triploid Crassostrea virginica (Gmelin, 1791) Grow Faster Than Diploids but are Equally Susceptible to Perkinsus marinus (1991). Journal of Shellfish Research, 10(2), 445–450.

https://scholarworks.wm.edu/vimsarticleshttps://scholarworks.wm.edu/vimsarticles/1277 (accessed 16 August 2023)

Butler, P. A., 1949. Gametogenesis in the oyster under conditions of depressed salinity. The Biological Bulletin, 96(3), 263–269. https://doi.org/10.2307/1538361

Butts, I. A. E., Babiak, I., Ciereszko, A., Litvak, M. K., Słowińska, M., Soler, C., Trippel, E. A., 2011. Semen characteristics and their ability to predict sperm cryopreservation potential of Atlantic cod, Gadus morhua L. Theriogenology, 75(7), 1290–1300. https://doi.org/10.1016/J.THERIOGENOLOGY.2010.11.044

Clements, J. C., Carver, C. E., Mallet, M. A., Comeau, L. A., Mallet, A. L., 2021. CO2-induced low pH in an eastern oyster (Crassostrea virginica) hatchery positively affects reproductive development and larval survival but negatively affects larval shape and size, with no intergenerational linkages: . ICES Journal of Marine Science, 78(1), 349–359. https://doi.org/10.1093/icesjms/fsaa089

Coen, L. D., Brumbaugh, R. D., Bushek, D., Grizzle, R., Luckenbach, M. W., Posey, M. H., Powers, S. P., Tolley, S. G., 2007. Ecosystem services related to oyster restoration. Source: Marine Ecology Progress Series, 341, 303–307. https://doi.org/10.2307/24871847

Cosson, J., Groison, A. L., Suquet, M., Fauvel, C., Dreanno, C., Billard, R., 2008. Studying sperm motility in marine fish: an overview on the state of the art. Journal of Applied Ichthyology, 24(4), 460–486. https://doi.org/10.1111/J.1439-0426.2008.01151.X

Dong, Q. X., Eudeline, B., Allen, S. K., Dong, B., Dong, Q. O., Eudeline, B., Tiersch, T. R., 2002. Factors Affecting Sperm Motility of Tetraploid Pacific Oysters Factors Affecting Sperm Motility of Tetraploid Pacific Oysters. VIMS Articles, 469. https://scholarworks.edu/vimsarticles/469 (accessed 16 August 2023)

Dridi, S., Salah Romdhane B, M'hamed Elcafsi, M., 2006. Seasonal variation in weight and biochemical composition of the Pacific oyster, Crassostrea gigas in relation to the gametogenic cycle and environmental conditions of the Bizert lagoon, Tunisia. https://doi.org/10.1016/j.aquaculture.2006.10.028

Faulk, C. K., Holt, G. J., 2005. Advances in rearing cobia Rachycentron canadum larvae in recirculating aquaculture systems: Live prey enrichment and greenwater culture. Aquaculture, 249(1–4), 231–243. https://doi.org/10.1016/J.AQUACULTURE.2005.03.033

Folch, J., Lees, M., Sloane, G. H., 1957. A simple method for the isolation and purification of total lipids from animal tissues. J. Biol Chem. 226 497-507. https://doi.org/10.1016/S0021-9258(18)64849-5

Franco, A., Heude Berthelin, C., Goux, D., Sourdaine, P., Mathieu, M., 2008. Fine structure of the early stages of spermatogenesis in the Pacific oyster, Crassostrea gigas (Mollusca, Bivalvia). Tissue & Cell, 40(4), 251–260. https://doi.org/10.1016/J.TICE.2007.12.006

Fuhrmann, M., Petton, B., Quillien, V., Faury, N., Morga, B., Pernet, F., 2016. Salinity influences disease-induced mortality of the oyster Crassostrea gigas and infectivity of the ostreid herpesvirus 1 (OsHV-1). Aquaculture Environment Interactions, 8, 543–552. https://doi.org/10.3354/AEI00197

Gallager, S. M., & Mann, R.,1986. Growth and survival of larvae of Mercenaria mercenaria (L.) and Crassostrea virginica (Gmelin) relative to broodstock conditioning and lipid content of eggs. Aquaculture, 56(2), 105–121. https://doi.org/10.1016/0044-8486(86)90021-9

Glandon, H., Michaelis, A., Politano, V., Alexander, S., Vlahovich, E., Reece, K., Koopman, H., Meritt, D., Paynter, K., 2016. Impact of Environment and Ontogeny on Relative Fecundity and Egg Quality of Female Oysters (Crassostrea virginica) from Four Sites in Northern Chesapeake Bay. 1691.

https://scholarworks.wm.edu/vimsarticleshttps://scholarworks.wm.edu/vimsarticles/1691

Gobler, C. J., Talmage, S. C., & Cooke, S., 2014. Physiological response and resilience of early life-stage Eastern oysters (Crassostrea virginica) to past, present and future ocean acidification. 2. https://doi.org/10.1093/conphys/cou004

Gregory, K. M., McFarland, K., Hare, M. P., 2023. Reproductive Phenology of the Eastern Oyster, Crassostrea virginica (Gmelin, 1791), Along a Temperate Estuarine Salinity Gradient. Estuaries and Coasts, 46(3), 707–722. https://doi.org/10.1007/S12237-022-01163-W/TABLES/8

Grice R., Tarnecki A., 2023. Alabama Shellfish Aquaculture Situation & outlook report: Production Year 2022. Alabama Cooperative Extension System. https://www.aces.edu/blog/topics/aquaculture/alabama-shellfish-aquaculture-situation-outlook-report-production-year-2022/ (accessed 16 August 2023)

Grice R., 2023. List of Operating Farms. Alabama oyster Aquaculture. https://alaquaculture.com/state/ (accessed 16 August 2023)

Guo, X., DeBrosse, G. A., Allen, S. K.,1996. All-triploid Pacific oysters (Crassostrea gigas Thunberg) produced by mating tetraploids and diploids. Aquaculture, 142(3–4), 149–161. https://doi.org/10.1016/0044-8486(95)01243-5

Guo, X., Wang, Y., Xu, Z., Yang, H., 2009. Chromosome set manipulation in shellfish. New Technologies in Aquaculture: Improving Production Efficiency, Quality and Environmental Management, 165–194. https://doi.org/10.1533/9781845696474.1.165

IPCC, 2022: Summary for Policymakers [H.-O. Pörtner, D.C. Roberts, E.S. Poloczanska, K. Mintenbeck, M. Tignor, A. Alegría, M. Craig, S. Langsdorf, S. Löschke, V. Möller, A. Okem (eds.)]. In: Climate Change 2022: Impacts, Adaptation and Vulnerability. Contribution of Working Group II to the Sixth Assessment Report of the Intergovernmental Panel on Climate Change [H.-O. Pörtner, D.C. Roberts, M. Tignor, E.S. Poloczanska, K. Mintenbeck, A. Alegría, M. Craig, S. Langsdorf, S. Löschke, V. Möller, A. Okem, B. Rama (eds.)]. Cambridge University Press, Cambridge, UK and New York, NY, USA, pp. 3–33, https://doi.org/10.1017/9781009325844.001

JunPeng, D., ZhaoPing, W., YuTing, C., YangChun, L., Yang, Y., PengFei, L., YiQun, L., 2018. Effects of salinity on Crassostrea angulata sperm quality and fertilization using PI/Rh123 dual fluorescent staining and flow cytometry. Journal of Fisheries of China, 42(11), 1737–1746. https://doi.org/10.11964/jfc.20180211171

Kennedy, V. S. 1996. The ecological role of the eastern oyster, Crassostrea virginica, with remarks on disease. Oceanographic Literature Review, 12(43), 1251.

https://www.infona.pl//resource/bwmeta1.element.elsevier-3a3f8861-19fd-3c84-b062-0cdf1cceca11

Kooijman, S. A. L. M., 2009. Dynamic energy budget theory for metabolic organisation, third edition. Dynamic Energy Budget Theory for Metabolic Organisation, Third Edition, 1–514. https://doi.org/10.1017/CBO9780511805400

Lango-Reynoso, F., Chávez-Villalba, J., Cochard, J. C., le Pennec, M., 2000. Oocyte size, a means to evaluate the gametogenic development of the Pacific oyster, Crassostrea gigas (Thunberg). Aquaculture, 190(1–2), 183–199. https://doi.org/10.1016/S0044-8486(00)00392-6

La Peyre, M. K., Eberline, B. S., Soniat, T. M., La Peyre, J. F., 2013. Differences in extreme low salinity timing and duration differentially affect eastern oyster (Crassostrea virginica) size class growth and mortality in Breton Sound, LA. Estuarine, Coastal and Shelf Science, 135, 146–157. https://doi.org/10.1016/J.ECSS.2013.10.001

Lavaud, R., La Peyre, M. K., Casas, S. M., Bacher, C., La Peyre, J. F., 2017. Integrating the effects of salinity on the physiology of the eastern oyster, Crassostrea virginica, in the northern Gulf of Mexico through a Dynamic Energy Budget model. Ecological Modelling, 363, 221–233. https://doi.org/10.1016/J.ECOLMODEL.2017.09.003

MacKenzie, C.L. Jr., Burrell, V. G. Jr., Rosenfield A., Hobart, W. L. (eds.)., 1997. The history, present condition, and future of the molluscan fisheries of North and Central America and Europe, Volume 1, Atlantic and Gulf Coasts. U.S. Dep. Commer., NOAA Tech. Rep.127, p1-14. https://spo.nmfs.noaa.gov/sites/default/files/tr127opt.pdf (accessed 16 August 2023)

Magaña-Carrasco, A., Brito-Manzano, N., Gómez-Vázquez, A., Cruz Hernández, A., 2018. Effects of temperature and salinity on inducing spawning in the eastern oyster (Crassostrea

virginica) under laboratory conditions. Ecosistemas y Recursos Agropecuarios, 5(14), 239–246. https://doi.org/10.19136/ERA.A5NL4.1236

Mai, H., Gonzalez, P., Pardon, P., Tapie, N., Budzinski, H., Cachot, J., Morin, B., 2014. Comparative responses of sperm cells and embryos of Pacific oyster (Crassostrea gigas) to exposure to metolachlor and its degradation products. Aquatic Toxicology, 147, 48–56. https://doi.org/10.1016/j.aquatox.2013.11.024

Manley, J., Power, A., Walker, R., 2008. Wild Eastern Oyster, Crassostrea virginica, spat collection for commercial grow-out. Univeristy of Georgia Marine Extension Service, 2.

Massapina, C., Joaquim, S., Matias, D., & Devauchelle, N., 1999. Oocyte and embryo quality in Crassostrea gigas (Portuguese strain) during a spawning period in Algarve, South Portugal. Aquatic Living Resources, 12(5), 327-333. https://doi.org/10.1016/S0990-7440(99)00115-1

McCarty, A. J., McFarland, K., Small, J., Allen, S. K., Plough, L., 2020. Heritability of acute low salinity survival in the Eastern oyster (Crassostrea virginica). Aquaculture, 529, 735649. https://doi.org/10.1016/J.AQUACULTURE.2020.735649

Mcfarland, K., Donaghy, L., Volety, A. K., 2013. Effect of acute salinity changes on hemolymph osmolality and clearance rate of the non-native mussel, Perna viridis, and the native oyster, Crassostrea virginica, in Southwest Florida. Aquatic Invasions, 8, 299–310. https://doi.org/10.3391/ai.2013.8.3.06

McFarland, K., Vignier, J., Standen, E., Volety, A., 2022. Synergistic effects of salinity and temperature on the eastern oyster Crassostrea virginica throughout the lifespan. Marine Ecology Progress Series, 700, 111–124. https://doi.org/10.3354/meps14178

McFarland, K., Vignier, J., Standen, E., & Volety, A. K., 2022. Synergistic effects of salinity and temperature on the eastern oyster Crassostrea virginica throughout the lifespan. Marine Ecology Progress Series, 700, 111–124. https://doi.org/10.3354/MEPS14178

Monteforte, M., Garcia-Gasca, A., 1994. Spat collection studies on pearl oysters Pinctada mazatlanica and Pteria sterna (Bivalvia, Pteriidae) in Bahia de La Paz, South Baja California, Mexico. Hydrobiologia, 291, 21–34. https://doi.org/10.1007/BF00024236

Moore, J. F., Pine, W. E., Frederick, P. C., Beck, S., Moreno, M., Dodrill, M. J., Boone, M., Sturmer, L., Yurek, S., 2020. Trends in Oyster Populations in the Northeastern Gulf of Mexico: An Assessment of River Discharge and Fishing Effects over Time and Space. Marine and Coastal Fisheries, 12(3), 191–204. https://doi.org/10.1002/mcf2.10117

Morrison, W. R., Smith, L. M., 1964. Preparation of fatty acid methyl esters and dimethylacetals from lipids with boron fluoride methanol. Journal Lipid Research, 5, 600–608. https://doi.org/10.1016/S0022-2275(20)40190-7

Murawski, S. A., Kilborn, J. P., Bejarano, A. C., Chagaris, D., Donaldson, D., Hernandez, F. J., MacDonald, T. C., Newton, C., Peebles, E., Robinson, K. L., 2021. A Synthesis of Deepwater Horizon Impacts on Coastal and Nearshore Living Marine Resources. Frontiers in Marine Science, 7. https://doi.org/10.3389/fmars.2020.594862

Myers, J. N., Nichols, Z. G., Abualreesh, M. H., El Husseini, N., Taylor, Z. A., Coogan, M. P., Gurbatow, J., Vo, K. M., Zadmajid, V., Chatakondi, N., Dunham, R. A., Butts, I. A. E., 2020. Impact of sperm density on hatch success for channel catfish (Ictalurus punctatus) ♀ × blue catfish (Ictalurus furcatus) ♂ hybrid production. Aquaculture, 521, 735024. https://doi.org/10.1016/J.AQUACULTURE.2020.735024

National Marine Fisheries Service, 2022. Fisheries of the United States. (2020). U.S. Department of Commerce, NOAA Current Fishery Statistics No. 2020. https://www.fisheries.noaa.gov/national/sustainable-fisheries/fisheries-united-states (accessed 16 August 2023)

[Database] NOAA Fisheries Office of Science and Technology, Commercial Landings Query, www.fisheries.noaa.gov/foss (accessed 16 August 2023)

Nell, J. A., 2002. Farming triploid oysters. Aquaculture, 210(1–4), 69–88. https://doi.org/10.1016/S0044-8486(01)00861-4

Nichols, Z. G., Rikard, S., Mohammad, S., Alavi, H., Walton, W. C., Butts, I. A. E., 2021. Regulation of sperm motility in Eastern oyster (Crassostrea virginica) spawning naturally in seawater with low salinity. PLoS ONE 16(3): e0243569. https://doi.org/10.1371/journal.pone.0243569

Perales-Valdivia, H., Sanay-González, R., Valle-Levinson, A., 2018. Effects of tides, wind and river discharge on the salt intrusion in a microtidal tropical estuary. Regional Studies in Marine Science, 24, 400–410. https://doi.org/10.1016/J.RSMA.2018.10.001

Perchec, G., Jeulin, C., Cosson, J., Andre, F., Billard, R., 1995. Relationship between sperm atp content and motility of carp spermatozoa. Journal of Cell Science, 108(2), 747–753. https://doi.org/10.1242/JCS.108.2.747

Prein, A. F., Rasmussen, R. M., Ikeda, K., Liu, C., Clark, M. P., Holland, G. J., 2017. The future intensification of hourly precipitation extremes. Nature Climate Change, 7(1), 48–52. https://doi.org/10.1038/nclimate3168

Piferrer, F., Beaumont, A., Falguière, J.-C., Flajšhans, M., Haffray, P., Colombo, L., 2009. Polyploid fish and shellfish: Production, biology and applications to aquaculture for

performance improvement and genetic containment. Aquaculture, 293, 125–156. https://doi.org/10.1016/j.aquaculture.2009.04.036

Posadas, B.C., 2022. The Growing U.S Oyster Aquaculture Industry. Mississippi MarketMaker Newsletter, Vol. 12, No. 6. http://extension.msstate.edu/newsletters/mississippi-marketmaker/2022/vol-12-no6-the-growing-us-oyster-aquaculture-industry (Accessed 16 August 2023)

Pourmozaffar, S., Tamadoni Jahromi, S., Rameshi, H., Sadeghi, A., Bagheri, T., Behzadi, S., Gozari, M., Zahedi, M. R., Abrari Lazarjani, S., 2020. The role of salinity in physiological reponses of bivalves. Reviews in Aquaculture, 12(3), 1548–1566. https://doi.org/10.1111/RAQ.12397

Rodríguez-Jaramillo, C., García-Corona, J. L., Zenteno-Savín, T., Palacios, E., 2022. The effects of experimental temperature increase on gametogenesis and heat stress parameters in oysters: Comparison of a temperate-introduced species (Crassostrea gigas) and a native tropical species (Crassostrea corteziensis). Aquaculture, 561, 738683. https://doi.org/10.1016/J.AQUACULTURE.2022.738683

Rurangwa, E., Kime, D. E., Ollevier, F., Nash, J. P., 2004. The measurement of sperm motility and factors affecting sperm quality in cultured fish. Aquaculture, 234(1–4), 1–28. https://doi.org/10.1016/J.AQUACULTURE.2003.12.006

Rurangwa, E., Volckaert, F. A. M., Huyskens, G., Kime, D. E., Ollevier, F., 2001. Quality control of refrigerated and cryopreserved semen using computer-assisted sperm analysis (CASA), viable staining and standardized fertilization in African catfish (Clarias gariepinus). Theriogenology, 55(3), 751–769. https://doi.org/10.1016/S0093-691X(01)00441-1

Sadri, S., Khoei, A. J., 2023. Ambient salinity affects silver nanoparticles (AgNPs) induced toxicity in the marine bivalve, the rock oyster, Saccostrea cucullata. Aquaculture Reports, 30, 101596. https://doi.org/10.1016/J.AQREP.2023.101596

Schneider, C. A., Rasband, W. S., Eliceiri, K. W., 2012. NIH Image to ImageJ: 25 years of image analysis. Nature Methods, 9(7), 671–675. https://doi.org/10.1038/nmeth.2089

Shpigel, M., Barber, B. J., Mann, R., 1992. Effects of elevated temperature on growth, gametogenesis, physiology, and biochemical composition in diploid and triploid Pacific oysters, Crassostrea gigas Thunberg. Journal of Experimental Marine Biology and Ecology, 161(1), 15–25. https://doi.org/10.1016/0022-0981(92)90186-E

Shumway, S.E., 1996. Natural Environmental Factors. In: Kennedy VS, Newell RIE, Eble AF, editors. The Eastern Oyster Crassostrea virginica. Maryland Sea Grant College, College Park, Maryland; pp. 467–513. https://repository.library.noaa.gov/view/noaa/45763 (accessed 16 August 2023)

Sies, H., 1993. Strategies of antioxidant defense. European Journal of Biochemistry, 215(2), 213–219. https://doi.org/10.1111/J.1432-1033.1993.TB18025.X

Song, Y. P., Suquet, M., Quéau, I., Lebrun, L., 2009. Setting of a procedure for experimental fertilisation of Pacific oyster (Crassostrea gigas) oocytes. Aquaculture, 287(3-4), 311–314. https://doi.org/10.1016/j.aquaculture.2008.10.018

Soudant, P., Marty, Y., Moal, J., Robert, R., Quéré, C., Le Coz, J. R., Samain, J. F., 1996a. Effect of food fatty acid and sterol quality on Pecten maximus gonad composition and reproduction process. Aquaculture, 143(3–4), 361–378. https://doi.org/10.1016/0044-8486(96)01276-8

Soudant, P., Moal, J., Marty, Y., Samain, J. F., 1996b. Impact of the quality of dietary fatty acids on metabolism and the composition of polar lipid classes in female gonads of Pecten

maximus (L.). Journal of Experimental Marine Biology and Ecology, 205(1–2), 149–163. https://doi.org/10.1016/S0022-0981(96)02608-1

Spilke, J., Piepho, H. P., Hu, X., 2005. Analysis of Unbalanced Data by Mixed Linear Models Using the mixed Procedure of the SAS System. Journal of Agronomy and Crop Science, 191(1), 47–54. https://doi.org/10.1111/J.1439-037X.2004.00120.X

Stanley, J. G., Allen, S. K., Hidu, H., 1981. Polyploidy induced in the American oyster, Crassostrea virginica, with cytochalasin B. Aquaculture, 23(1–4), 1–10. https://doi.org/10.1016/0044-8486(81)90002-8

Subasinghe, M. M., Jinadasa, B. K. K. K., Navarathne, A. N., Jayakody, S., 2019. Seasonal variations in the total lipid content and fatty acid composition of cultured and wild Crassostrea madrasensis in Sri Lanka. Heliyon, 5(2), 1238. https://doi.org/10.1016/j.heliyon.2019.e01238

Sühnel, S., José Lagreze-Squella, F., Legat, J. F. A., Puchnick-Legat, A., Strand, Å., Sühnel Lagreze, S., Manoel Rodrigues de Melo, C., 2023. Effects of Salinity on the Reproductive Cycle of the Mangrove Oyster Crassostrea tulipa in Hatchery Conditions. Aquaculture Research, 2023, 1–12. https://doi.org/10.1155/2023/7409585

Sussarellu, R., Suquet, M., Thomas, Y., Lambert, C., Fabioux, C., Pernet, M. E. J., Goïc, N. Le, Quillien, V., Mingant, C., Epelboin, Y., Corporeau, C., Guyomarch, J., Robbens, J., Paul-Pont, I., Soudant, P., Huvet, A., 2016. Oyster reproduction is affected by exposure to polystyrene microplastics. Proceedings of the National Academy of Sciences of the United States of America, 113(9), 2430–2435. https://doi.org/10.1073/PNAS.1519019113/SUPPL_FILE/PNAS.1519019113.SD03.XLS

Thanormjit, K., Chueycham, S., Phraprasert, P., Sukparangsi, W., Kingtong, S., 2020. Gamete
characteristics and early development of the hooded oyster Saccostrea cuccullata (Born,
1778). Aquaculture Reports, 18, 100473. https://doi.org/10.1016/J.AQREP.2020.100473

Walton, W. C., Swann, L., 2021. Role of Sea Grant in Establishing Commercial Oyster
Aquaculture through Applied Research and Extension. Journal of Contemporary Water
Research & Education, 174(1), 171–179. https://doi.org/10.1111/j.1936-704x.2021.3367.x

Whyte, J. N. C., Bourne, N., Ginther, N. G., 1990. Biochemical and energy changes during
embryogenesis in the rock scallop Crassadoma gigantea. Marine Biology, 106(2), 239–244.
https://doi.org/10.1007/BF01314806/METRICS

Whyte, J. N. C., Bourne, N., Ginther, N. G., 1991. Depletion of nutrient reserves during
embryogenesis in the scallop Patinopecten yessoensis (Jay). Journal of Experimental Marine
Biology and Ecology, 149(1), 67–79. https://doi.org/10.1016/0022-0981(91)90117-F

Yang, H., Simon, N., Sturmer, L. N., 2018. Production and Performance of Triploid Oysters for
Aquaculture: FA208, 7/2018. EDIS, 2018(4). https://doi.org/10.32473/EDIS-FA208-2018

Zanette, J., de Almeida, E. A., da Silva, A. Z., Guzenski, J., Ferreira, J. F., Di Mascio, P.,
Marques, M. R. F., Bainy, A. C. D., 2011. Salinity influences glutathione S-transferase
activity and lipid peroxidation responses in the Crassostrea gigas oyster exposed to diesel oil.
Science of The Total Environment, 409(10), 1976–1983.
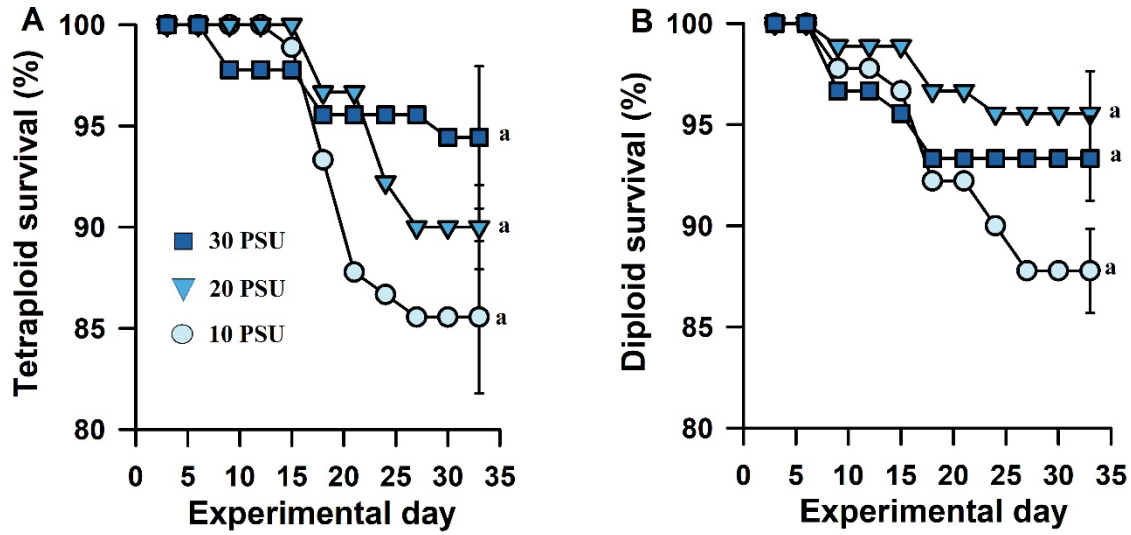https://doi.org/10.1016/J.SCITOTENV.2011.01.048

Figure 1.1 Survival of tetraploid (A) and diploid (B) Eastern oyster (*Crassostrea virginica*) broodstock held at 10, 20, and 30 PSU over a 30-day experimental trial. One-way ANOVA was used to compare survival between the salinity treatments after 30 days. Means for each ploidy were contrasted using the Tukey-Kramer method and salinity treatments with the same letters were not significantly different ($P > 0.05$). Bars represent least square means ± standard error.
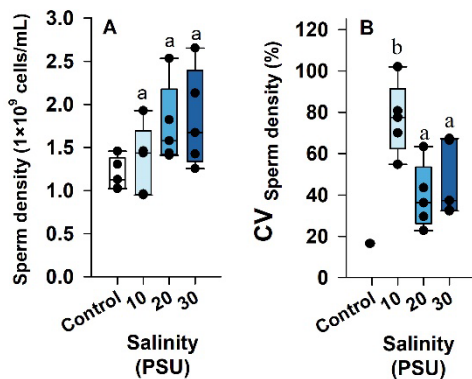
Figure 1.2 Effect of holding salinity (10, 20, and 30 PSU) on sperm density (A) and male-to-male variation in density (B) (measured as coefficient of variation; CV) in tetraploid Eastern oyster (*Crassostrea virginica*). One-way ANOVA was used to compare density between salinity treatments after 3 days of holding. Box heights indicate interquartile range, horizontal line within box indicates median and mean, whiskers show minimum and maximum value within data, and dots represent individual values. Means were contrasted using the Tukey-Kramer method and salinity treatments with same letters were not significantly different ($P > 0.05$). Bars represent least square means ± standard error. The control represents 5 oysters sampled at the beginning of the trial.
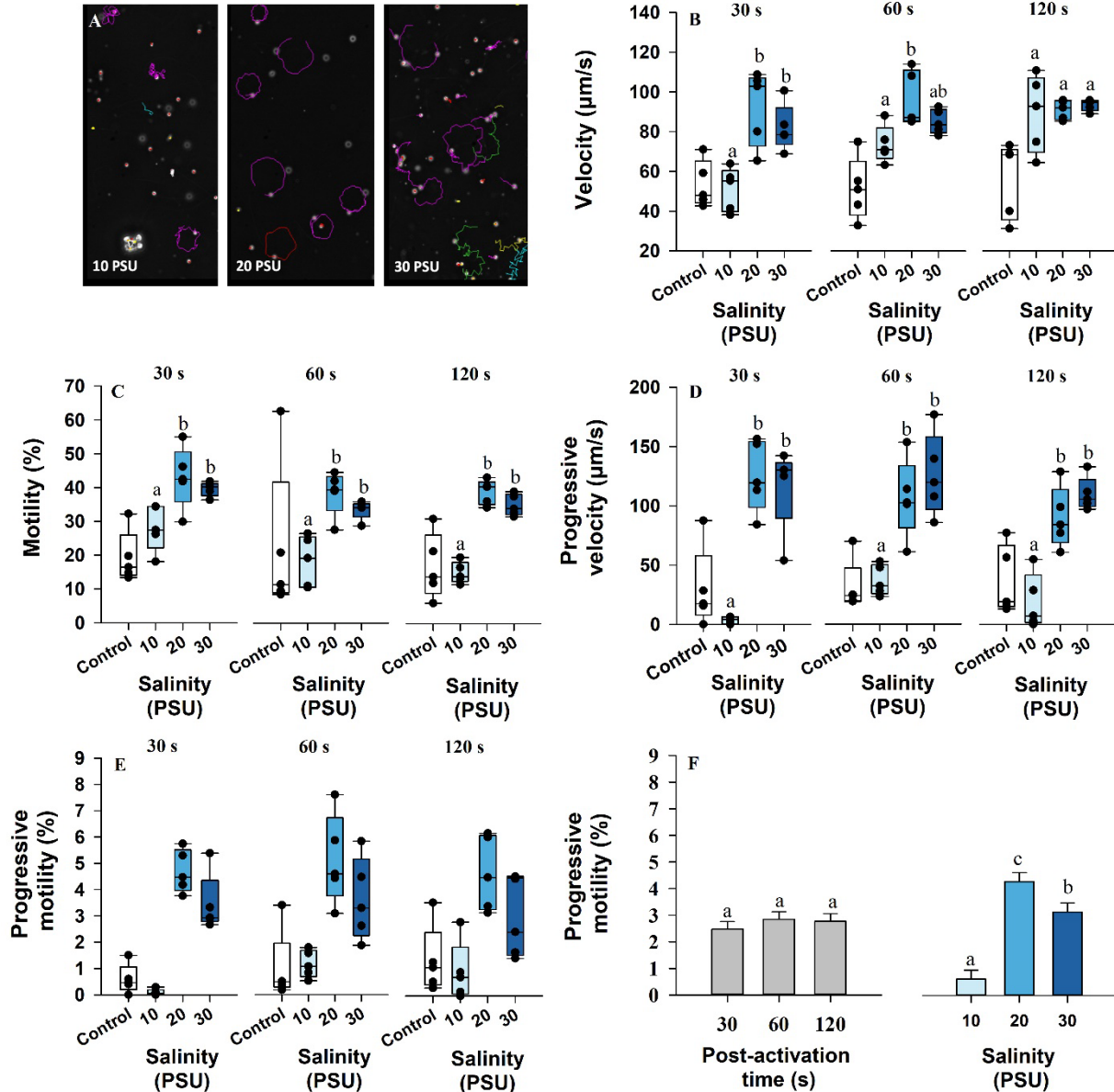
Figure 1.3 Effect of holding salinity (10, 20, and 30 PSU) on sperm kinematics in tetraploid Eastern oyster (*Crassostrea virginica*). Digital images of sperm head trajectories at each holding salinity are shown (A). Computer Assisted Sperm Analysis was used to determine the impact of holding salinity on sperm curvilinear velocity (VCL; B), percent motility (C), progressive VCL (D), and progressive motility (E-F) at 30, 60, and 120 s post activation. If a significant time post-activation × holding salinity interaction was detected, separate ANOVA models were run at each time-post-activation to determine salinity effects (B-

D). Main effects were interpreted when an interaction was non-significant (E-F). Box heights indicate interquartile range, horizontal line within box indicates median and mean, whiskers show minimum and maximum value within data, and dots represent individual values (A-E). Means were contrasted using the Tukey-Kramer method and salinity treatments with same letters were not significantly different ($P > 0.05$). Bars represent least square means ± standard error. The control represents 5 oysters sampled at the beginning of the trial.
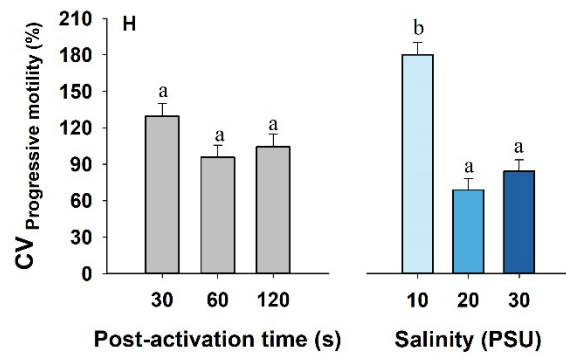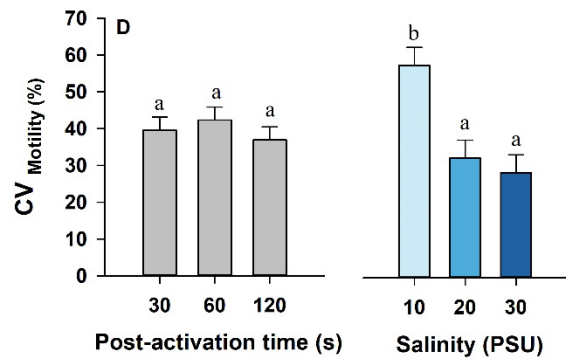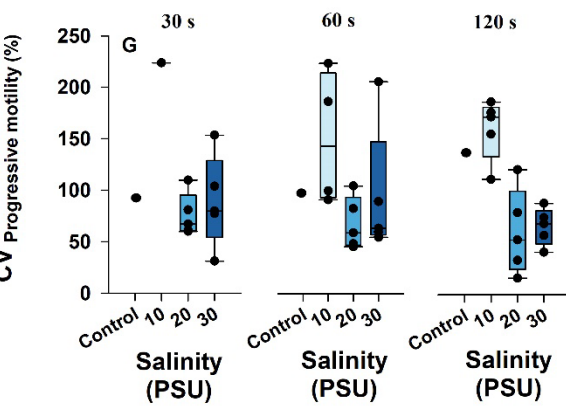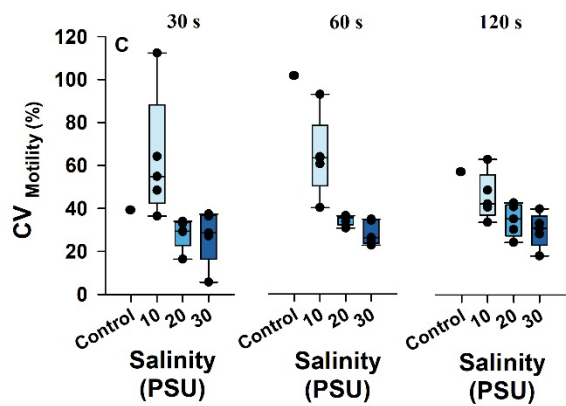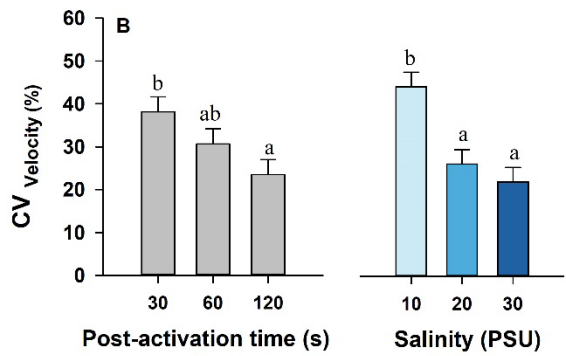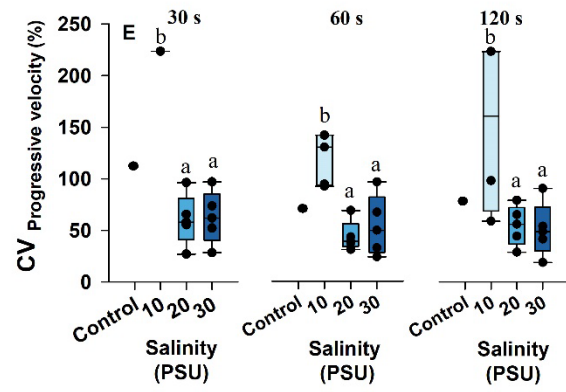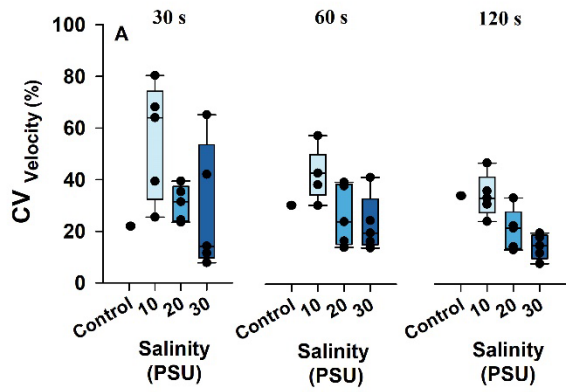
Figure 1.4 Effect of holding salinity (10, 20, and 30 PSU) on male-to-male variation (measured as coefficient of variation; CV) in sperm kinematics in tetraploid Eastern oyster (*Crassostrea virginica*). Computer Assisted Sperm Analysis was used to determine impact of holding salinity on CV in sperm curvilinear velocity (VCL; A-B), percent motility (C-D), progressive VCL (E-F), and progressive motility (G-H) at 30, 60, and 120 s post activation. If a significant time post-activation × holding salinity interaction was detected, separate ANOVA models were run at each time-post-activation to determine salinity effects (E-F). Main effects were interpreted when an interaction was non-significant (A-D,G-H). Box heights indicate interquartile range, horizontal line within box indicates median and mean, whiskers show minimum and maximum value within data, and dots represent individual values (A-E). Means were contrasted using the Tukey-Kramer method and salinity treatments with same letters were not significantly different (P > 0.05). Bars represent least square means ± standard error. The control represents 5 oysters sampled at the beginning of the trial.

Figure 1.5 Flow cytometry (A; dot plots shown) was used to determine the effect of holding salinity (10, 20, and 30 PSU) on sperm membrane viability (B) and male-to-male variation in viability (C) (measured as coefficient of variation; CV) in tetraploid Eastern oyster (*Crassostrea virginica*). One-way ANOVA was used to compare viability between salinity treatments after 30 days of holding. Box heights indicate interquartile range, horizontal line within box indicates median and mean, whiskers show minimum and maximum value within data, and dots represent individual values. Means were contrasted using the Tukey-Kramer method and salinity treatments with same letters were not significantly different (P > 0.05). Bars represent least square means ± standard error. The control represents 5 oysters sampled at the beginning of the trial.
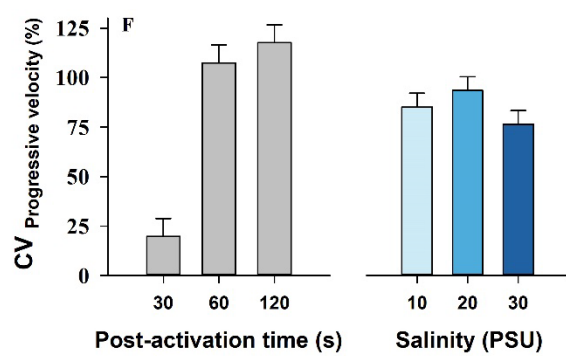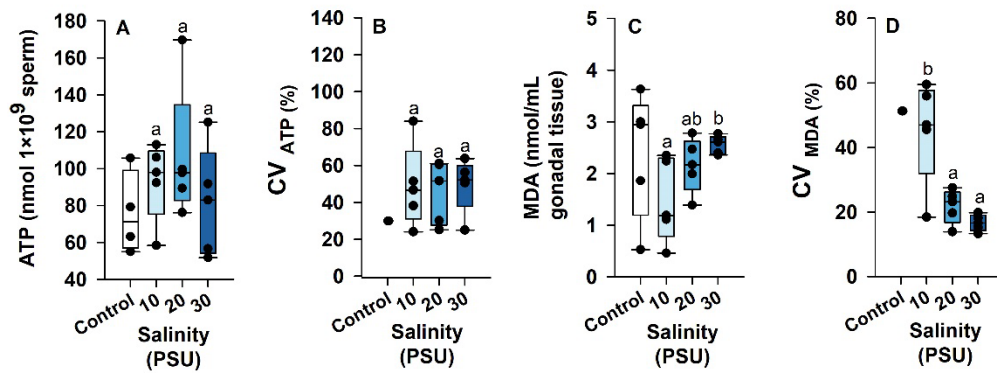
Figure 1.6 Effect of holding salinity (10, 20, and 30 PSU) on sperm adenosine 5′-triphosphate (ATP) concentration, (A) male-to-male variation in ATP (B) (measured as coefficient of variation; CV), oxidative stress (represented by malondialdehyde; MDA) and male-to-male variation in MDA (D) in tetraploid Eastern oyster (*Crassostrea virginica*). One-way ANOVA was used to compare ATP and MDA between salinity treatments after 30 days of holding. Box heights indicate interquartile range, horizontal line within box indicates median and mean, whiskers show minimum and maximum value within data, and dots represent individual values. Means were contrasted using the Tukey-Kramer method and salinity treatments with same letters were not significantly different (P > 0.05). Bars represent least square means ± standard error. The control represents 5 oysters sampled at the beginning of the trial.
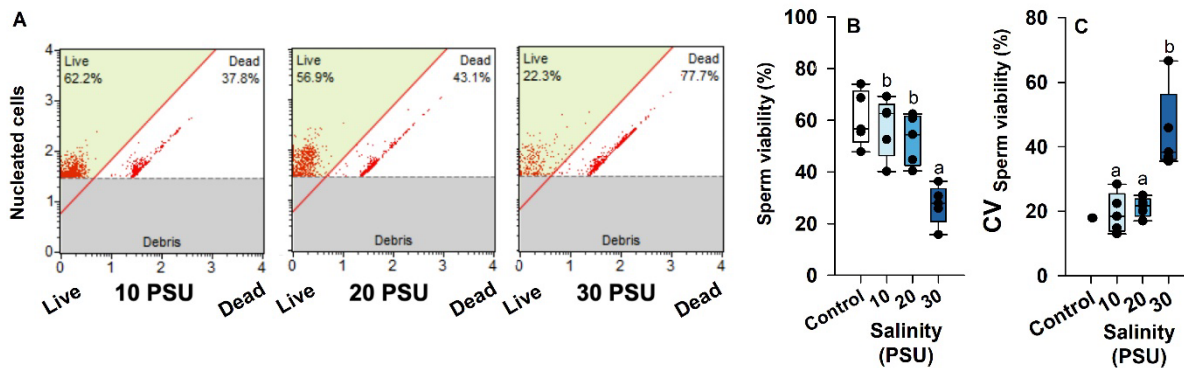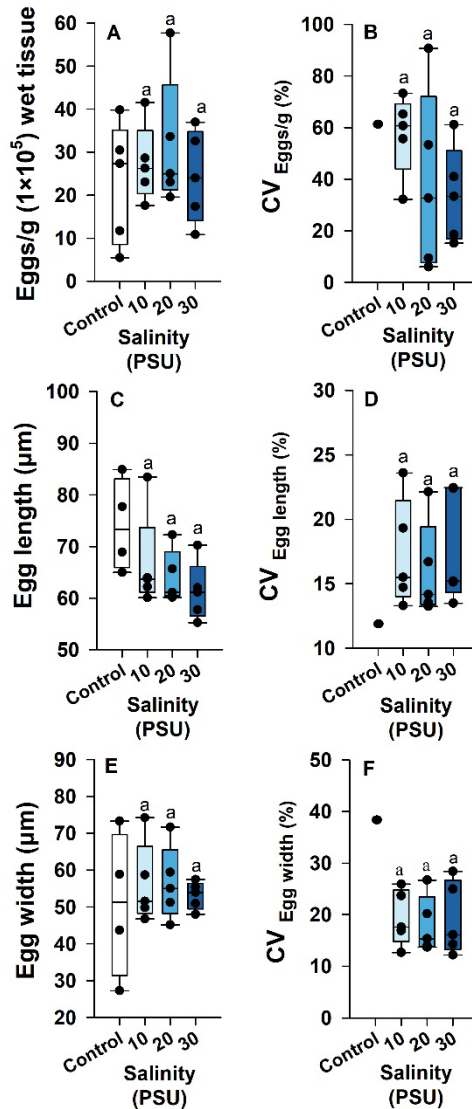
Figure 1.7 Effect of holding salinity (10, 20, and 30 PSU) on egg density, (A) female-to-female variation in density (B) (measured as coefficient of variation; CV), egg length (C), female-to-female variation in egg length (D), egg width (E), and female-to-female variation in egg length (F) in diploid Eastern oyster (*Crassostrea virginica*). One-way ANOVA was used to compare egg traits between salinity treatments after 30 days of holding. Box heights indicate interquartile range, horizontal line within box indicates median and mean, whiskers show minimum and maximum value within data, and dots represent individual values. Means were contrasted using the Tukey-Kramer method and salinity treatments with same letters were not

significantly different (P > 0.05). Bars represent least square means ± standard error. The control represents 5 oysters sampled at the beginning of the trial.
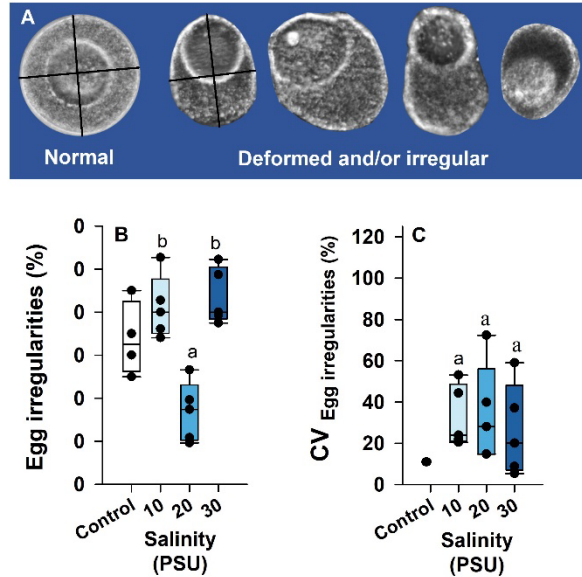
Figure 1.8 Effect of holding salinity (10, 20, and 30 PSU) on egg irregularities (A-B) and female-to-female variation in egg irregularities (C) (measured as coefficient of variation; CV) in diploid Eastern oyster (*Crassostrea virginica*). One-way ANOVA was used to compare egg irregularities between salinity treatments after 30 days of holding. Box heights indicate interquartile range, horizontal line within box indicates median and mean, whiskers show minimum and maximum value within data, and dots represent individual values. Means were contrasted using the Tukey-Kramer method and salinity treatments with same letters were not significantly different (P > 0.05). Bars represent least square means ± standard error. The control represents 5 oysters sampled at the beginning of the trial. Black lines indicate length and width measurements.

Table 1.1 Composition of fatty acids (mg/g dry weight) extracted from male tetraploid Eastern oyster (*Crassostrea virginica*) gonad tissue after 30 days at holding salinity.

Fatty acid	Control	10 PSU			20 PSU			30 PSU			F^2	*P*
	Mean	Mean	SD	SEM[1]	Mean	SD	SEM[1]	Mean	SD	SEM[1]		
14:0	10.28	9.16	2.21	0.99	8.15	2.15	0.96	7.74	1.85	0.83	0.50	0.616
15:0	2.55	2.35	0.44	0.20	2.20	0.45	0.20	2.03	0.33	0.15	0.65	0.538
16:0	54.00	50.63	6.35	2.84	46.99	7.53	3.37	42.78	5.17	2.31	1.74	0.217
17:0	2.16	2.33	0.24	0.11	2.21	0.31	0.14	2.08	0.15	0.07	1.30	0.308
18:0	4.54	4.95	0.32	0.14	4.46	0.53	0.24	4.43	0.44	0.20	2.13	0.162
16:1n7	12.58	11.48	2.52	1.13	10.23	2.39	1.07	9.94	1.83	0.82	0.51	0.615
18:1n9	10.58	10.24	1.07	0.48	9.38	1.45	0.65	9.27	1.67	0.75	0.79	0.475
18:1n7	6.37	5.71	0.66	0.30	5.31	0.73	0.33	4.76	0.52	0.23	2.64	0.112
22:1n11	0.20	0.32	0.14	0.06	0.29	0.16	0.07	0.23	0.12	0.06	0.42	0.665
20:1n9	2.75	2.92	0.24	0.11	2.78	0.29	0.13	2.60	0.17	0.08	2.44	0.130
16:2n4	1.40	1.34	0.32	0.15	1.21	0.26	0.12	1.19	0.20	0.09	0.36	0.703
16:3n4	4.73	4.49	1.12	0.50	4.35	1.35	0.60	3.83	0.85	0.38	0.38	0.689
18:2n6	7.27	6.93	1.08	0.48	6.31	1.28	0.57	5.69	0.95	0.43	1.42	0.280
18:3n6	1.05	0.83	0.20	0.09	0.73	0.24	0.11	0.67	0.17	0.07	0.67	0.531
18:3n4	0.35	0.34	0.06	0.03	0.33	0.08	0.04	0.31	0.06	0.02	0.20	0.821
18:3n3	9.69	9.32	1.83	0.82	8.19	1.87	0.84	7.39	1.43	0.64	1.32	0.303
18:4n3	19.99	17.80	4.22	1.89	15.70	4.03	1.80	14.36	2.98	1.33	0.88	0.439
20:2n6	0.66	0.60	0.07	0.03	0.61	0.10	0.04	0.56	0.04	0.02	0.53	0.602
20:3n6	1.18	0.94	0.15	0.07	0.89	0.13	0.06	0.84	0.08	0.04	0.62	0.553
20:4n6 (ARA)	5.45	5.25	0.98	0.44	5.10	0.93	0.41	4.43	0.59	0.26	1.20	0.335
20:3n3	1.01	0.69	0.20	0.09	0.70	0.15	0.07	0.64	0.12	0.06	0.18	0.841
20:4n3	2.10	1.78	0.38	0.17	1.64	0.29	0.13	1.42	0.28	0.12	1.59	0.244
20:5n3 (EPA)	56.47	50.52	10.79	4.82	45.84	10.30	4.61	40.34	7.16	3.20	1.22	0.328
22:4n6	0.61	0.63	0.14	0.06	0.62	0.16	0.07	0.46	0.07	0.03	2.69	0.108
22:5n6	1.47	1.60	0.23	0.10	1.53	0.25	0.11	1.37	0.11	0.05	1.49	0.264
22:5n3	2.50	2.47	0.57	0.26	2.25	0.44	0.19	1.98	0.17	0.08	1.52	0.259
22:6n3 (DHA)	60.09	50.96	8.90	3.98	47.79	9.41	4.21	41.49	5.99	2.68	1.63	0.237
total n-3	79.02	133.54	26.55	11.87	122.10	26.18	11.71	107.61	17.86	7.99	1.32	0.304
total n-6	11.58	16.77	2.58	1.15	15.79	2.89	1.29	14.02	1.85	0.83	1.47	0.269
n-3/n-6	6.82	7.92	0.52	0.23	7.69	0.47	0.21	7.65	0.28	0.13	0.56	0.587
Total SFA	86.70	69.42	9.32	4.17	64.01	10.87	4.86	59.06	7.62	3.41	1.41	0.281
Total MUFA	26.47	30.68	4.34	1.94	27.99	4.86	2.18	26.81	3.94	1.76	0.94	0.419
Total PUFA	83.95	156.48	30.42	13.61	143.79	30.59	13.68	126.96	20.65	9.24	1.28	0.315

ARA = arachidonic acid; EPA = eicosapentaenoic acid; DHA = docosahexaenoic acid

[1] Values are means ± SEM (n = 5)

[2] Numerator degrees of freedom = 2; denominator degrees of freedom = 12

Table 1.2 Composition of fatty acids (mg/g dry weight) extracted from female diploid Eastern oyster (*Crassostrea virginica*) gonad tissue after 30 days at holding salinity. Bold indicates a row with statistically different values.

Fatty acid	Control Mean	10 PSU Mean	10 PSU SD	10 PSU SEM[1]	20 PSU Mean	20 PSU SD	20 PSU SEM[1]	30 PSU Mean	30 PSU SD	30 PSU SEM[1]	F[2]	P
14:00	12.09	13.56	3.56	1.59	11.69	3.13	1.4	8.97	1.17	0.52	3.27	0.073
15:00	1.8	**1.75[b]**	**0.2**	**0.09**	**1.60[ab]**	**0.3**	**0.13**	**1.34[a]**	**0.08**	**0.04**	**5.07**	**0.025**
16:00	45.32	**47.48[b]**	**3.81**	**1.7**	**43.87[ab]**	**5.14**	**2.3**	**38.49[a]**	**3.31**	**1.48**	**6.32**	**0.013**
17:00	1.92	2.03	0.13	0.06	1.9	0.18	0.08	1.76	0.16	0.07	3.75	0.054
18:00	4.52	5.65	0.57	0.25	5.28	0.74	0.33	4.94	0.63	0.28	1.54	0.254
16:1n7	15.89	15.18	3.79	1.69	13.55	2.99	1.34	11.17	0.94	0.42	2.21	0.153
18:1n9	10.59	**11.18[b]**	**0.82**	**0.37**	**10.61[ab]**	**0.59**	**0.26**	**9.57[a]**	**0.82**	**0.37**	**5.84**	**0.017**
18:1n7	6.77	7.3	0.87	0.39	6.65	0.69	0.31	6.24	0.42	0.19	2.87	0.096
22:1n11	0.23	0.29	0.08	0.04	0.28	0.08	0.03	0.28	0.03	0.01	0.01	0.994
20:1n9	3.1	**3.24[b]**	**0.24**	**0.11**	**3.10[ab]**	**0.27**	**0.12**	**2.79[a]**	**0.29**	**0.13**	**3.88**	**0.05**
16:2n4	0.96	**1.06[b]**	**0.16**	**0.07**	**0.93[ab]**	**0.17**	**0.08**	**0.78[a]**	**0.05**	**0.02**	**5.77**	**0.018**
16:3n4	3.06	3.22	1.18	0.53	2.3	0.9	0.4	1.77	0.28	0.13	2.84	0.098
18:2n6	5.26	**5.78[b]**	**0.54**	**0.24**	**5.18[ab]**	**0.68**	**0.3**	**4.56[a]**	**0.31**	**0.14**	**6.76**	**0.011**
18:3n6	0.56	**0.60[b]**	**0.13**	**0.06**	**0.51[ab]**	**0.1**	**0.04**	**0.43[a]**	**0.03**	**0.01**	**4.43**	**0.036**
18:3n4	0.28	0.29	0.03	0.01	0.26	0.05	0.02	0.24	0.02	0.01	2.18	0.156
18:3n3	5.75	**6.49[b]**	**1.07**	**0.48**	**5.48[ab]**	**1.26**	**0.56**	**4.45[a]**	**0.37**	**0.17**	**6.05**	**0.015**
18:4n3	10.12	10.65	2.88	1.29	8.49	3	1.34	6.6	0.51	0.23	3.65	0.058
20:2n6	0.52	0.53	0.05	0.02	0.49	0.09	0.04	0.49	0.06	0.03	0.63	0.551
20:3n6	0.6	0.61	0.07	0.03	0.54	0.11	0.05	0.48	0.04	0.02	3.18	0.078
20:4n6 (ARA)	2.82	**3.00[b]**	**0.33**	**0.15**	**2.81[ab]**	**0.44**	**0.2**	**2.35[a]**	**0.2**	**0.09**	**5.27**	**0.023**
20:3n3	0.47	0.42	0.04	0.02	0.37	0.1	0.05	0.35	0.04	0.02	1.73	0.219
20:4n3	1.53	1.57	0.09	0.04	1.42	0.3	0.13	1.22	0.18	0.08	3.59	0.06
20:5n3 (EPA)	27.17	**29.13[b]**	**5.59**	**2.5**	**25.55[ab]**	**5.49**	**2.45**	**20.75[a]**	**1.08**	**0.48**	**4.64**	**0.032**
22:4n6	0.69	0.66	0.06	0.03	0.67	0.07	0.03	0.67	0.2	0.09	0.02	0.976
22:5n6	1.13	1.29	0.1	0.04	1.32	0.12	0.05	1.15	0.12	0.05	3.32	0.071
22:5n3	1.71	**1.98[b]**	**0.21**	**0.09**	**1.73[ab]**	**0.21**	**0.09**	**1.54[a]**	**0.15**	**0.07**	**6.61**	**0.012**
22:6n3 (DHA)	32.28	**33.67[b]**	**3.55**	**1.59**	**29.77[ab]**	**3.84**	**1.72**	**26.38[a]**	**1.96**	**0.88**	**6.62**	**0.012**
total n-3	79.02	**83.90[b]**	**12.88**	**5.76**	**72.81[ab]**	**14.03**	**6.27**	**61.29[a]**	**3.77**	**1.68**	**5.44**	**0.021**
total n-6	11.58	12.47	1.07	0.48	11.5	1.5	0.67	10.13	0.92	0.41	4.96	0.027
n-3/n-6	6.82	6.7	0.52	0.23	6.29	0.4	0.18	6.07	0.33	0.15	2.77	0.102
Total SFA	86.7	70.47	7.99	3.57	64.34	9.04	4.04	55.5	5.06	2.27	5.27	0.023
Total MUFA	26.47	37.19	5.35	2.39	34.19	4.41	1.97	30.05	2.27	1.02	3.52	0.063
Total PUFA	83.95	100.94	15.26	6.82	87.8	16.58	7.41	74.21	4.78	2.14	5.37	0.022

ARA = arachidonic acid; EPA = eicosapentaenoic acid; DHA = docosahexaenoic acid

[1] Values are means ± SEM (n = 5)

[2] Numerator degrees of freedom = 2; denominator degrees of freedom = 12
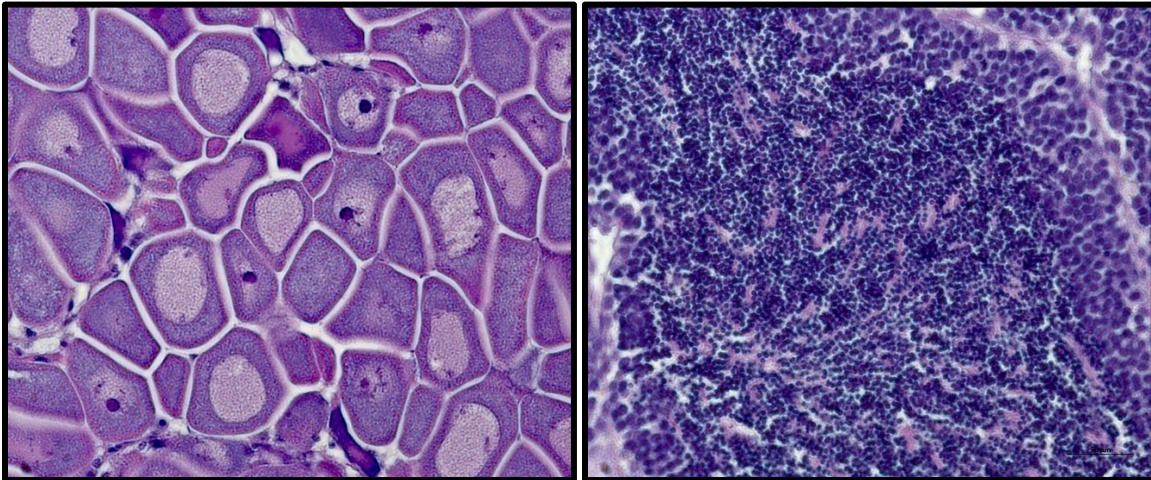
[3] Values in the same bold row with different superscripts are different ($P < 0.05$)

Chapter 2

Impact of seasonality on reproductive physiology of diploid and tetraploid

Eastern oyster, *Crassostrea virginica*

V. MacKenzie Tackett., Jim A. Stoeckel., F. Scott Rikard., Andrea M. Tarnecki., Ian A.E. Butts.,

Impact of seasonality on reproductive physiology of diploid and tetraploid Eastern oyster,

Crassostrea virginica. To be Submitted to *M.E.P.S.* in December 2023

2.1 Abstract

Eastern oyster is grown in estuaries and reliant on abiotic cues to produce gametes. However, limited knowledge is available on their reproductive biology, including the gametogenic cycle. The aim was to quantify monthly changes in gametogenesis and gamete quality for male tetraploid and female diploid Eastern oyster in the Gulf of Mexico (GoM) from June 2022 to July 2023. Monthly changes in temperature and salinity were recorded. Shell morphometrics and sex was determined. Sperm density, sperm activity, the Spermatogenic Maturity Index (SMI), and gonad coverage area were determined. Oocyte diameter, the Oogenesis Maturity Index (OMI), and gonad coverage area were quantified. Temperature ranged from 5.4-34.9°C and salinity ranged from 4.8-29.8 PSU. Shell morphometrics increased over the annual cycle. When gametes were detectable, 48-80% of tetraploids and 45-70% of diploids were males. Hermaphrodites were identified in both ploidies in June; an additional tetraploid was identified in March. Sperm density exhibited monthly fluctuations with highest densities in June-July, September, and April-May. Sperm were motile when present, with highest motility in June-July. The highest sperm velocity was recorded in June-July and March-May. Tetraploids exhibited the highest SMI from June-September and April-May with increased variability in December-January. Mature sperm cells were predominant in tetraploids in June-July. Gonadal coverage was highest from June-September and March-May. OMI was highest from June-September and March-May, while variability was highest from August-March. Largest oocyte diameters and gonad coverage area were observed in June-July and April-May. Together, these findings provide novel insights into reproductive dynamics for Eastern oyster in GoM.

2.2 Introduction

Estuaries are critical natural habitats for birds, mammals, fish, and invertebrate species (NOAA, 2021). These regions can provide a buffer zone, where sediment and pollutants are filtered out of runoff water before entering open ocean waters (Burchard et al., 2018; López et al., 2021). Additionally, within the United States, 47% of the gross domestic product (Rouleau et al., 2021) and 75% of the commercial fish catch (NOAA, 2021) come from estuary regions. This comes as no surprise, as most of the fish and shellfish in the United States spend at least one of their life stages in estuaries. However, due to their geographical locations, these regions are particularly vulnerable to shifts in abiotic factors due to climate change, like temperature and salinity (USEPA, 1999; IPCC, 2022; Leal Filho et al., 2022). Current climate predictions indicate that extreme weather events and temperatures will continue to increase in the United States over the next 50 years (IPCC, 2022). Studies have already indicated that climate change has increased surface temperatures in the Southeastern United States, specifically in the Gulf of Mexico (GoM: Wang et al., 2023). The Gulf Coast is also facing an increase in frequency and severity of precipitation events (Brown et al., 2019). Weather events coupled with an increase in river discharge have caused salinity fluctuations and salinity extremes in GoM estuaries (Prein et al., 2017). These changes have already begun to negatively impact many of the commercial species that rely on these crucial regions. Unfortunately, these effects are likely to worsen in the next 50 years (IPCC, 2022).

The Eastern oyster, *Crassostrea virginica*, is native to benthic habitats along the Atlantic coast of America from Canada to the GoM, the Caribbean, and the coast of South America (Kennedy et al., 1996). It is a keystone species with many ecological services and economic value (NMFS, 2022). As ecosystem engineers, oysters are a vital component of benthic communities in estuarine

systems, especially in the GoM (Coen et al., 2007; La Peyre et al., 2019; NMFS, 2022). However, the combination of climate change and overharvesting has drastically reduced natural populations over the last fifteen years (Kennedy, 1996; Moore et al., 2020). In Alabama, the pre-2008 oyster harvest averaged ~850,000 pounds annually, but by the end of that same year, the harvest had declined to slightly over 70,000 pounds (NOAA Fisheries Office of Science and Technology, 2023). Although regulatory changes in wild harvest practices have facilitated a resurgence in both natural oyster populations and the industry, a complete recovery remains distant. Ongoing restoration initiatives are currently underway with the primary objective of revitalizing historical reef locations. Furthermore, the continually expanding aquaculture industry in the region has provided supplementary relief to natural reefs by supplying large volumes of oysters to the commercial market. Notably, in 2019, the GoM aquaculture sector surpassed all other United States coasts in shellfish production by volume (NMFS, 2022).

As market demands continue to rise, farmers have introduced polyploidy manipulation into hatchery production (Barber et al., 1992). While oysters naturally occur as diploid (2n), additional chromosomal pairs can be retained during embryonic development resulting in polyploidy (Guo et al., 2009). Several forms of polyploidy exist, including triploid (3n) organisms, which possess one additional set of chromosomes, and tetraploid (4n) organisms which contain two additional pairs (Piferrer et al., 2009). Specific characteristics of triploids, like more consistent meat quality in summer spawning months, make them more desirable than their diploid counterparts (Yang et al., 2018). Additionally, triploid oysters typically exhibit faster growth as less energy is dedicated to reproduction, consequently reaching market size sooner than diploids (Barber and Mann, 1991), again making them a superior choice for farming.

Over time, techniques to induce polyploidy have resulted in the development of tetraploid broodstock. The cross between male tetraploids and female diploids produces 100% triploid offspring, while previous methods were less successful and had higher mortality rates (Guo et al., 1996; Yang et al., 2018; Guo et al., 2009). Producing and maintaining tetraploid broodstock has not come without its challenges. Tetraploid and diploid larvae have been shown to have differing survival rates which is especially evident in the early generations of tetraploid lineages where survival is low (Yang et al., 2019). In these same generations, growth rates and the onset of sexual maturity are slower than typically seen in young diploids (Yang et al., 2019). However, there is a lack of information regarding tetraploid reproduction.

Determining when broodstock are ripe and ready to spawn is a key aspect of the triploid production process. As diploid oysters typically exhibit a cyclical reproductive trend in the GoM, stages of gametogenesis can be classified based on histological observations and the size and shape of gametes (Thompson et al., 1996). While there is no complete agreement as to how many stages should be used, image analysis can be utilized to quantitatively analyze sperm and oocyte development within gonad tissues (Lango-Reynoso et al., 2000; Fabioux et al., 2005). As males progress through gametogenesis, cells become smaller and more specialized; conversely, as females progress, cells become larger as they develop their necessary components (Eckelbarger and Davis, 1996a, 1996b). Once temperatures and development are in the optimal stage, gametes are released into the water column, and the remaining gametes are reabsorbed into the tissues (Thompson et al., 1996). Utilizing histological images to measure cell development offers an easily understandable dataset to quantify development in both sperm and oocyte cells, as well as the homogeneity of the gonad (Tomkiewicz et al., 2011). Additionally, histological images can be used to quantify the body composition of Eastern oyster to determine the percentage of tissue dedicated

to gonad development throughout an annual cycle (Quintana et al., 2011). Also, combining quantitative histology with percentage-based data associated with gonad coverage area can provide a more comprehensive picture regarding the reproductive ability of the individual (Quintana et al., 2011).

Farmers generally rely on environmental cues to condition and determine spawning times for both tetraploid and diploid broodstock (Wallace et al., 2008). Oyster spawning generally occurs in warmer months, where in the GoM water temperatures that exceed 20°C can induce spawning (Nelson, 1928: Gregory et al., 2023). However, when housing tetraploid and diploid broodstock in proximity, spawn containment can be a concern. Unplanned spawns between tetraploids and diploids can produce triploid offspring, subsequently negatively impacting natural populations (Gong et al., 2004). While mitigation programs currently exist to avoid unplanned spawning, fully understanding the reproductive cues and cycles of tetraploid broodstock can aid in the prevention of unwanted spawning. Triploid (Gregory et al., 2023) and diploid (Eckelbarger and Davis, 1996a, 1996b) reproductive cycles have been studied, but there is a gap in available information regarding tetraploid Eastern oyster gametogenesis. Not only would this information aid in the prevention of unwanted spawning but would also allow farmers to fully capitalize on triploid production.

As external broadcast spawners, it is important for Eastern oyster gametes to be healthy upon release. Studies have shown that spat survival is largely dependent on the health of the gametes used in their production (Gallager and Mann, 1986; Vignier et al., 2017). Sperm health can easily be defined as the cell's ability to fertilize and produce a viable embryo, which is largely impacted by environmental conditions and cell development (Bobe and Labbé, 2009; Boulais et al., 2017). As sperm is released into the water column motility is activated and has limited time to reach a viable oocyte (Rurangwa et al., 2004; Song et al., 2009). In Eastern oyster, swimming kinetics,

such as motility and velocity (VCL; Boulais et al., 2019; Nichols et al., 2021), are indicative of sperm quality, which can be quantified using Computer Assisted Sperm Analysis (CASA) software (Rurangwa et al., 2001; Cosson et al., 2008). While sperm quality is quantifiable, there are few commonly used predictive markers for oyster oocytes. Oocyte size has been used as a metric to determine oocyte quality, although not without controversy (Boulais et al., 2015).

Thus, the aim of this study was to quantify monthly changes in gametogenesis for tetraploid male and diploid female oysters. Additionally, we aim to quantify gamete quality over an annual cycle to determine times of peak performance for each ploidy type. Understanding when each ploidy produces the healthiest and most viable gametes can help farmers understand natural spawning dynamics and optimize aquaculture production.

2.3 Materials and Methods

2.3.1 Oyster culture and experimental design

Tetraploid (n = 240, spawned 6/3/2020) and diploid (n = 240, spawned 7/7/2020) oysters used in this study were produced and reared at the Auburn University Shellfish Lab (AUSL) on Dauphin Island. Oysters were held in adjustable longline systems in Grand Bay, AL (30.3749090ºN, -88.3145984ºW). Mesh baskets (12.5 mm; BST Oyster Supplies, Cowell, South Australia) were attached to adjustable monofilament cables strung between two pilings ~100 m apart with PVC riser posts every ~3 m. The monofilament cables were adjusted to accommodate water column fluctuations and keep baskets fully submerged. Baskets were filled halfway with oysters; if the volume exceeded half, the oysters were split into two baskets to provide appropriate space. As baskets accumulated fouling, oysters were placed into clean baskets. Two-year-old diploid and tetraploid oysters were held over the course of one year (1 June 2022 to 1 May 2023). Oysters were held in the same environmental conditions to determine the effect of ploidy on the annual

gametogenic cycle. Data loggers (YSI multiparameter sonde, EXCO 3, YSI Inc., Yellow Springs, OH, USA) were launched at the long line site in Grand Bay, AL ~1 m above the sea floor. Probes were exchanged and cleaned monthly to prevent the buildup of biofouling. Temperature and salinity were recorded every 15 min from 1 June 2022 to 1 May 2023 to determine hourly means. During the first week of each month, 20 oysters per ploidy were randomly collected from baskets and transported to AUSL. All oysters were scrubbed to remove bio-fouling materials and transported, on ice (~4°C), to the Aquatic Reproductive Physiology Laboratory (ARPL) at Auburn University, Auburn, AL (32.6526°N, -85.4859°W).

2.3.2 Data collection

2.3.2.1 Sex determination and morphology

After arrival at ARPL, a precision standard balance (TS200-02; Ohaus Corporation, NJ, USA) and digital calipers (VWR, Item number 12777-830, PA, USA) were used to collect morphometric data. This included weight ($\pm$ 0.01 g), length ($\pm$ 0.03 mm), width ($\pm$ 0.03 mm), and height ($\pm$ 0.03 mm). Each month a minimum of 10 oysters were opened per ploidy. If 5 male tetraploids and 5 female diploids were not identified within the first 10 oysters, additional oysters were sampled until the appropriate sample size was reached. A maximum of 20 oysters were opened per ploidy per month. Oysters were opened at the hinge using a shucking knife, with the left valve resting on the table. After releasing the hinge, the adductor muscle was severed from the right valve to fully open the oyster. All tools were cleaned with 90% ethanol between individuals. Mantle tissue was thoroughly rinsed of excess salt water with deionized water. The remaining liquid was blotted dry with Kim wipes. A 1 μL sample of gonad was then taken from each oyster and sex was determined using a Zeiss Axiolab 5 microscope (Carl Zeiss Microscopy, LLC, NY, USA) equipped with 20×

negative phase objective (SAF "A-Plan" 20x/0.45 Ph-n1). Oysters were categorized as males, females, hermaphrodites, or unknown. Monthly sex ratios were then calculated.

2.3.2.2 Sperm quality analysis

Cell density

Semen was collected from tetraploid males through shallow slices in the gonadal tissue created with a sterile 20-gauge scalpel. Digestive tissue was avoided during the collection process. Semen samples were collected with 1,000 µL pipette tips, deposited in 1.5 µL microcentrifuge tubes, and kept at 19°C in an Echotherm™ Chilling/Heating Dry Bath (Torrey Pines Scientific, CA, USA) for the duration of the experiment. In cases where sperm were activated, the respective sample was disposed of, and an alternative individual was utilized. Non-activated sperm were diluted using Artificial Salt Water (ASW; 516 mM NaCl, 10.4 mM KCl, 11 mM $CaCl_2 \times 2H_2O$, 34 mM $MgCl_2$ $\times 6H_2O$, 22 mM $MgSO_4 \times 7H_2O$; Boulais et al., 2018). Dilutions ranged from 0 to 400× depending on initial densities. Sperm density (cells/mL) was quantified for each male, in duplicate, using a Neubauer hemocytometer following Myers et al. (2020). In brief, once sperm were diluted in ASW, samples were homogenized for ~10 s, and 10 µL of homogenate was pipetted onto the hemocytometer. Sperm settled onto a 5×5 grid (1 mm^2), where sperm inside five squares (0.2 mm^2; top left, top right, bottom right, bottom left, and center) were counted. To determine the average cell density of the diluted sperm, all counts were summed and multiplied by 5 to estimate the number of sperm cells in the entire grid. The dilution factor was multiplied by the sperm density in the 5×5 grid and multiplied by 10,000 (to identify cells/ mL).

Swimming kinematics

Sperm activation solution was prepared with 516 mM NaCl, 10.4 mM KCl, 11 mM $CaCl_2$, 34 mM $MgCl_2$, and 22 mM $MgSO_4$ (Nichols et al., 2021b) and salinity of the final solution adjusted from 40 PSU to 20 PSU with ultrapure water (Milli-Q® Advantage A10 Water Purification System, Merck Kagan, Darmstadt, Germany). Pluronic F-127 (0.4%; Sigma Aldrich, MO, USA) was added to prevent cells sticking to glass slides. Activation solution was buffered to ~7.5 pH with 20 mM Tris. Activation solution (99 to 399 µL) was pipetted into 1.5 mL microcentrifuge tubes and placed into a 19°C Echotherm™ Chilling/Heating Dry Bath. To activate sperm motility, roughly 1.0 µL of semen was diluted into prefilled microcentrifuge tubes and rapidly inverted several times to mix thoroughly. Immediately, 5 µL of activated sperm were pipetted into a 20 µm deep 2X-CEL chamber (Hamilton Thorne Biosciences, MA, USA), under a light microscope (AXIOlab 5, listed above). Motility was recorded in triplicate at 20× magnification (20×) at 30, 60, and 120 s post-activation for each male. Motile sperm (%) and curvilinear velocity (VCL; µm/s) were determined using CASA software (CEROS II, Hamilton Thorne Biosciences, MA, USA). CASA Images were taken at 60 frames per s, exposure was set to 4 ms, and camera gain at 300. Cells were tracked between 3 and 11 µm, minimum cell brightness was set at 57, and the photometer range of illumination fields were between 55 and 65. All CASA videos were manually examined to verify accuracy following Butts et al. (2011). If software mistakenly split a single sperm track, combined crossing tracts of multiple sperm, or marked motile sperm as stagnant, tracks were removed from the analysis. Additionally, if sperm were drifting over the field of vision, rather than actively swimming, tracks were removed.

2.3.2.3 Histology and oocyte quality

All samples were processed according to Howard et al. (1983). In brief, 1 to 2 mm posterior of where the palps and gills meet, a 4 to 5 mm section was harvested perpendicular to the anterior-posterior axis. All tissue was placed in 10% phosphate-buffered formalin. After 24 h formalin was exchanged. Samples were held no longer than 12 weeks in formalin and formalin was exchanged once every 4 weeks. Preserved tissue was processed at the Scott-Ritchey Research Center, where samples were dehydrated using 70 to 100% ethanol solutions, embedded in paraffin, and sectioned to 5 μm. Sections were stained with hematoxylin and eosin. Digital images were taken using a Zeiss Imager.A2 microscope (Carl Zeiss Microscopy, LLC, White Plains, NY, USA) equipped with a 40× objective (A- Plan 40× / 0, 65 pH2) or Zeiss Discovery.V12 SteREO with a Zeiss Plan S 1.0× FWD 81 mm objective. Both scopes were equipped with a Zeiss Axio-cam 305 digital camera and Zen Pro v.6.1 software. For each oyster sampled (n = 5 tetraploid, n = 5 diploid), two tissue sections were placed on one slide, where 8 digital images were taken per tissue sectioned. If the tissue was too large for 2 sections per slide, 16 digital images were taken per tissue. Cells were organized according to maturity (Table 2.1 and 2.2) and relative area fraction (F) was estimated. The area fraction of different tissue was estimated by placing a grid, 48-point for males and 30-point for females, on all digital images using the ImageJ plugin "Analyze" (tetraploid males = 5 males × 12 months × 16 images × 48-point grid = 46,080 cells analyzed; diploid females = 5 females × 12 months × 16 images × 30-point grid = 28,800 cells analyzed). Progression of gonadal cells was assessed using a modified version of the Spermatogenic Maturity Index (SMI) (Tomkiewicz et al., 2011). This index ranged from 0 (oysters had connective tissue and excluded area) to 5 (oysters had fully developed gametes). More specifically, the category classification for males was, as follows: 0 = connective tissue and excluded area; 1 = spermatogonia (> 6.5 μm); 2

= primary spermatocytes (5.5 to 6.5 µm); 3 = secondary spermatocytes (4.5 to 5.5 µm); 4 = spermatids (3.5 to 4.5 µm); 5 = spermatozoa (< 3.5 µm). For females, the Oogenesis Maturity Inex (OMI) categories were, as follows: 0 = connective tissue and excluded area, 1 = follicular cells (< 5 µm), 2 = oogonia (5 to 15 µm), 3 = previtellogenic oocyte (15 to 25 µm), 4 = post-vitellogenic oocytes (25 to 40 µm), 5 = mature oocytes (> 40 µm). Additionally, mean oocyte diameters were determined each month for diploids utilizing cells from histological slides. Oocytes were measured at the widest point through the nucleus when present.

Histological slides were also utilized to measure the gonad coverage area for both males and females. Measurements were taken according to Quintana et al. (2011) to determine the proportion of tissue dedicated to gamete production. In brief, gametes for both males and females stain darker than other tissues, therefore color was used as an indicator to measure the gonad coverage and the body area. The ImageJ plugin "Analyze" was used to trace the inner and outer margins of the gonad (gonad coverage area) and a second measurement tracing the outer mantel (body area). Gonad coverage area was then divided by the body area to determine the percentage of gonad coverage area.

2.3.3 Statistics

All data were analyzed using SAS statistical analysis software (v. 9.1; SAS Institute Inc., Cary, NC, USA). Residuals were tested for normality (Shapiro–Wilk test) and homogeneity of variance (plot of residuals vs. predicted values). Shell morphometrics, sperm density, SMI, OMI, oocyte diameter, and VCL data were $\log_{10}$ transformed, while percent data, including coefficient of variation ($CV = \frac{\text{Standard deviation}}{\text{Sample mean}} \times 100$), gonad coverage area, and sperm motility were arcsine square-root transformed to meet assumptions of normality and homoscedasticity when necessary.

The Kenward–Roger procedure was used to approximate denominator degrees of freedom for all F-tests (Spilke et al., 2005). To examine the effect of month and time post-activation on sperm kinematic traits, data were analyzed using a series of repeated measures factorial ANOVA models. Each model contained month and post-activation time, as well as the corresponding month × post-activation time interaction. If a non-significant interaction was detected the main effects of month and time were interpreted. Mixed-model ANOVAs were used for shell morphology, sperm density, SMI, gonad coverage area, and oocyte diameter, to determine differences between months. Means were contrasted using the Tukey's test. Alpha was set at 0.05 for main effects and interactions. CVs were determined for SMI and OMI. A series of one-way ANOVA models were used to examine the degree of variability between sample months.

2.4 Results

2.4.1 Seasonal variation

Seasonal variation was recorded for temperature and salinity from 1 June 2022 to 1 May 2023. Daily mean temperature ranged from 5.4°C in December 2022 to 34.9°C in June 2022, while daily mean salinity ranged from 4.8 PSU in March 2023 to 29.8 PSU in November 2022 (Fig. 1A-B).

2.4.2 Sex determination and morphology

Total weight and morphometric traits increased throughout the *annual sampling period* in tetraploid males ($F_{11,44} \geq 21.66$; $P < 0.0001$; Fig. 2A-D) and diploid females ($F_{11,44} \geq 9.57$; $P < 0.0001$; Fig. 2E-H).

Monthly sex ratios are represented graphically for both tetraploid and diploid oysters (Fig. 3A-B). Aside from one hermaphrodite identified in June 2022, tetraploids showed balanced male-to-female sex ratios from June to September with 47.5 to 60% males each month. In October,

tetraploid males became more prevalent with 80% of individuals being male. Only one individual possessed identifiable gametes in November, which were male. No identifiable gametes were detected in tetraploids in December and January. Noticeable male gametes reemerged in February, however, most oysters remained unidentifiable. Females reemerged in March along with another hermaphrodite. Thereafter, males were more prevalent in April and a 52.6 to 47.4% male-to-female sex ratio was observed in May.

In diploids, males were more prevalent from June to September 2022 (60 to 70% males per month) while in October, more females were detected (64.3%). In November, one individual possessed no identifiable gametes while the rest were male. No gametes were identified in December and January. Male gametes reemerged in February, while one individual remained unidentifiable. A hermaphrodite was identified in March, and the male-to-female ratio was more balanced from March to May (45 to 50 % males per month).

2.4.3 Sperm quality

Cell density

Sperm density in tetraploid males significantly increased and decreased several times throughout the annual sampling period ($F_{7,32} = 4.46$, $P = 0.002$; Fig. 2.4). More specifically, the highest reported sperm densities were observed in June and July, followed by a significant decline in August. Sperm density once again significantly increased to the highest levels in September, leading to another decline in October. Oysters had no sperm from November to January. In February, only one male was identified and excluded from all statistical analysis. Sperm density increased in March and once again reached the highest densities reported in April and May.

Sperm swimming kinematics

Sperm were motile in all months where cells were present. Only one tetraploid male had motile sperm in February 2022; thus, February was excluded from statistical analyses. The month × post-activation time interaction was not significant for motility ($F_{14, 49.9}$ = 0.46, P = 0.944), therefore the main effects (month and post-activation time) were interpreted. Sperm motility changed throughout the annual sampling period ($F_{7,32.5}$ = 11.31, P < 0.0001; Fig. 2.5A), where tetraploid oysters had the highest motility in June and July. Sperm motility declined in August and then remained low throughout the sampling period. Sperm motility did not change between 30 and 120 s post-activation ($F_{2,41.4}$ = 0.03, P = 0.967; Fig. 2.5B).

Similarly, the month × time post-activation interaction was not significant for VCL ($F_{14,52.3}$ = 1.40, P = 0.187). Thus, the main effects of month and post-activation time were analyzed separately. Monthly sampling time impacted sperm VCL ($F_{7,32}$ = 13.90, P < 0.0001; Fig. 2.5C), where the fastest moving cells were detected in June and July 2022. Coinciding with sperm motility, a sharp decline in velocity was observed in August, however in March swimming speed increased to the highest VCL which continued through May. Sperm velocity remained constant from 30 to 120 s post-activation ($F_{2,45.5}$ = 2.03, P = 0.143; Fig. 2.5D).

2.4.4 Histology and oocyte quality

Histology stains and digital images were analyzed for tetraploid males from June 2022 to May 2023 (Fig. 2.6A-L). Changes in SMI were significant throughout the annual sampling period ($F_{11,48}$ = 31.73, P < 0.0001; Fig. 2.7A). The highest SMI values (i.e., oysters possessing more mature

cells) were reported from June to September 2022, followed by a decline in October. The lowest SMI values were reported in November to January. Thereafter, the SMI continued to rise, again reaching the highest values in April and May. Male-to-male variation (measured using CV) in SMI was significantly different between months ($F_{11,47} = 11.19$, $P < 0.0001$; Fig. 2.7B). Specifically, variation was lowest from June to November 2022. Thereafter, male-to-male variation increased in December and January, followed by another decline in February to May.

The changes in gonadal cell type ratios were also quantified throughout the annual sampling period (Fig. 2.7C). Fully mature sperm were predominant in June and July, where over half of cells identified were fully developed. Thereafter, the percentage of less developed cells increased in August while fully developed cells made up only 20% of cells analyzed. In September, cells matured, and spermatids represented 34% of all cell types. Connective tissue and excluded areas quickly overtook all other cell types in October, which continued until February, where primary and secondary spermatocytes began emerging and made up 20 and 15% of cell types, respectively. Cells continued to develop in March and into April when 40% of cells were mature sperm again. Another spike in connective tissue and excluded area (52%) appeared in May 2023 with 16 percent being fully mature sperm.

The gonadal coverage area was also significantly different throughout the annual sampling period ($F_{11,34.9} = 13.19$, $P < 0.0001$: Fig. 2.7D). June to September 2022 had the highest gonadal coverage area, which quickly diminished in October and remained low until January. Thereafter, the gonadal coverage area steadily increased and again reached the highest values from March to May.

Diploid histological stains and digital images were analyzed over the same annual sampling period (Fig. 2.8A-L). Female OMI was significantly different between months ($F_{11,48} = 75.03$, $P <$

0.0001; Fig. 2.9A). The highest OMI valves were reported from June to September. Following September, OMI declined and then steadily increased until, again, reaching the highest values in March to May 2023. Similarly, female-to-female variability (measured using CV) in OMI differed throughout the sampling period ($F_{11,48}$ = 4.47, P = 0.0001; Fig. 2.9B), however female variability was highest between August 2022 to March 2023.

Oocyte diameter varied throughout the annual cycle ($F_{11,44}$ = 99.79, P < 0.0001; Fig. 2.9C), where females sampled in June and July had the largest oocytes. This was followed by a series of increases and decreases until the oocytes again had the highest diameters in April and May.

Gonadal coverage area was also significantly different between months ($F_{11,38.8}$ = 36.71, P < 0.0001; Fig. 2.9D). Here, coverage area followed a similar trend as oocyte diameter with highest coverage area reported in June and July 2022 and April and May 2023.

2.5 Discussion

As an environmentally and economically important species, the influences climate change has on Eastern oyster reproduction is vital information for farmers. With the introduction of tetraploid brood stock into triploid production, understanding how broodstock respond to temperature and salinity fluctuation can optimize triploid production. The aim of this project was to analyze gonadal development of tetraploid male and diploid female Eastern oyster experiencing the same ecological conditions. Additionally, we aimed to quantify gamete health over an annual cycle to determine peak performance times for male tetraploids and female diploids.

Eastern oyster growth, survival, and reproduction are heavily influenced by temperature and salinity (Loosanoff and Davis, 1952; Lowe et al., 2017). While, oysters exhibit a wide temperature tolerance, their reproductive cycles are triggered by temperature increases (Shumway, 1996),

79

where gametogenesis takes place between 18 to 25°C and spawning occurs at over 20°C in the Gulf of Mexico (Nelson, 1928; Thompson et al., 1996). Based on the sperm traits observed in this study, the highest quality and quantity of tetraploid sperm was produced in June and July. However, as this project began at peak spawning times, we were unable to determine the environmental influences that occurred while these gametes were developing. It is likely that temperatures and salinity were within optimal ranges previous to these months which promoted healthy gametes. During June and July of 2022, mean monthly temperatures peaked, exceeding 30°C. Research has shown that temperatures above 30°C adversely affect physiological functions, such as heart rate and oxygen consumption in Eastern oyster (Marshall et al., 2021). The prolonged exposure to high temperatures over these two months likely caused thermal stress on all individuals in this study, which resulted in a dip in gamete quality in August 2022. This was represented by a sharp decline of sperm motility and velocity as well as a decrease in gonad area for females as well as smaller oocyte diameters. Additionally, thermal tolerance can be influenced by salinity levels where tolerance decreases as salinity decreases, however during these high temperatures the salinity means were nonlethal (Marshall et al., 2021). The lowest salinity levels were observed in December, coinciding with lower temperatures.

Here, we anticipated that male gametes would be identified in tetraploids before their female diploid counterpart. In suboptimal conditions male gametes are more likely to be produced as the energetic investment is lower than that of oocyte production (Thompson et al., 1996; Fabioux et al., 2005). This was validated in February 2023, as tetraploid males were identified while diploid females were not identified until the subsequent month. Additionally, research has shown that males are also more predominant in winter months, which was represented in these samples for both tetraploids and diploids with only males identified in November 2022 and February 2023

(Fabioux et al., 2005). Additionally, it is worth noting that of individuals sampled during winter months male gametes were identified in more diploids than in tetraploids. While it is not overly common to see hermaphrodites in Easter oyster, 3 individuals were identified during this study (Arias-De León et al., 2013). One tetraploid hermaphrodite was seen in June 2022, while the other two, one tetraploid and one diploid, were found in March 2023. Due to the time of year and temperature these individuals were likely switching from male to female in more favorable reproductive conditions (Thompson et al., 1996).

Sperm quality changed over the annual sampling period. The Eastern oyster spawning season in the GoM is said to be from March to October which coincides with optimal reproductive temperatures (Shumway, 1996). However, in this study sperm quality sharply declined after July 2022 with a resurgence of sperm density in September followed by another sharp decline in October. As gametogenesis depends on proper environmental conditions, including temperature and food availability, Eastern oyster can continuously produce gametes when environmental conditions are optimal (Arias-De León et al., 2013). Oysters sampled during August and October 2022 could have spawned recently causing the discrepancy in sperm quality. However, after July 2022 sperm motility and velocity fell and did not recover until the start of the next spawning cycle. Boulas et al (2017) suggests that spermatozoa velocity is related to its maturation stage during spermatogenesis, where more mature sperm can produce more ATP. During this study all sperm was strip spawned and therefore may have been mature according to our SMI index but still amassing ATP. Sperm motility was lower in April and May of 2023 than June and July, the previous year. Spermatogonia can be found with spermatozoa in a ripe gonad due to the continuous production during the oyster's reproductive cycle, which would have been collected during our sampling (Boulais et al., 2017). Due to spermatogonia being nonmotile these cells would have

contributed to the low motility seen during those months (Boulais et al., 2017). Previous studies with Crassostrea *gigas* have also reported tetraploid sperm to be less motile and slower than sperm collected from diploids of the same age (Suquet et al., 2010). SMI and gonad coverage areas followed similar trends to one another in 2022, where the highest reproductive activity for both was seen from June to September. The following year the gonad coverage area reached levels similar to the previous year in March while SMI was not comparable until April. This delay was likely due to a cold front in March, which brought water temperatures under gametogenic requirements (Thompson et al., 1996).

Overall male gametes, when present, had similar quality as reported in the literature (Suquet et al., 2010). As many factors go into choosing when to spawn broodstock, we feel it is also important to consider that while diploid males only require 500 sperm/oocyte to successfully fertilize eggs, the decreased performance seen in tetraploid sperm requires 5,000 sperm/oocyte (Thompson et al., 1996). With this in mind, both June and July 2022 would have produced the highest density of motile sperm, with the highest velocity, potentially offering the best chance to fertilize diploid oocytes for triploid production.

To the best of our knowledge this is the first study to quantify female diploid Eastern oyster gametogenesis using an Oogonia Maturity Index (OMI) based on cell sizes, as opposed to more commonly used stages such as "developing, spawning, and spent" (Gregory et al. 2023). In this study, the reproductive cycle for diploid females coincided with previously reported results (Thompson et al., 1996; Gregory et al., 2023). However, using quantitative data allows less room for subjective errors to be made when processing data. Female OMI and gonad coverage area followed similar trends in 2022, having the highest values from June to October. A decline was seen in the coverage area during August however it recovered in September. As oysters can

continuously produce gametes when environmental conditions are optimal, females likely spawned near the sampling point in August and produced additional gametes which were seen in September (Arias-De León et al., 2013). In 2023, OMI reached values comparable to the previous year in March with gonad coverage area following in April. An increase in the CV OMI from August to March was likely due to unspawned oocytes and the production of new oocytes the following season (Lango-Reynoso et al., 2000).

While not widely agreed upon (Boulais et al., 2015), oocyte diameter continues to be an easily accessible metric to determine the reproductive ability of female broodstock (Lango-Reynoso et al., 2000). In this study, oocyte diameter increased to the highest values in June and July 2022 and then again in April and May 2023. As oocytes develop, they amass the required elements, like lipids, to produce viable embryos as well as increase in size (Eckelbarger and Davis, 1996b). While size, is not able to predict lipid content within oocytes, it is able to be used to determine the stage of development the female is in (Lango-Reynoso et al., 2000; Boulais et al., 2015).

Females presented at least five months of high OMI, gonad coverage area, and oocyte diameter. As each female can produce millions of eggs during each spawn this is plenty of time for farmers to produce healthy triploid spat (Cox and Mann, 1996).

2.6 Conclusions

The Eastern oyster continues to be an ecologically and environmentally important species within the estuaries of the GoM. However, climate change has already begun to alter the temperature and salinity in these areas. To the best of our knowledge Eastern oyster tetraploid gametogenesis has not been fully investigated. Understanding how tetraploid and diploid broodstock produce gametes can help maximize triploid spat production and potentially minimize loss due to low gamete

quality. Here we would recommend spawning for tetraploid male with diploid females in the GoM after temperatures are between 18- 25°C to encourage gametogenesis and when salinity is within nondetrimental ranges (~ 20 PSU) to promote healthy gamete production.

2.7 References

Arias-De León, C., Lango-Reynoso, F., Chávez-Villalba, J., Castañeda-Chávez, M.R., Ramírez-Gutiérrez, S.C., 2013. Oocyte cohort analysis: reproductive patterns of Crassostrea virginica (Bivalvia) in tropical lagoons of the Gulf of Mexico. Invertebr Reprod Dev 57, 85–94. https://doi.org/10.1080/07924259.2012.674065

Barber, B., Mann, R., 1991. Sterile Triploid Crassostrea virginica (Gmelin, 1791) Grow Faster Than Diploids But Are Equally Susceptible To Perkinsus marinus (1991). J Shellfish Res 10, 445–450.

Barber, B.J., Mann, R., Allen, S.K., 1992. Optimization of triploid induction for the oyster Crassostrea virginica (Gmelin). Aquaculture 106, 21–26. https://doi.org/10.1016/0044-8486(92)90246-H

Bobe, J., Labbé, C., 2009. Egg and sperm quality in fish. Gen Comp Endocrinol 165, 535–548. https://doi.org/10.1016/j.ygcen.2009.02.011

Boulais, M., Corporeau, C., Huvet, A., Bernard, I., Quere, C., Quillien, V., Fabioux, C., Suquet, M., 2015. Assessment of oocyte and trochophore quality in Pacific oyster, Crassostrea gigas. Aquaculture 437, 201–207. https://doi.org/10.1016/j.aquaculture.2014.11.025

Boulais, M., Demoy-Schneider, M., Alavi, S.M.H., Cosson, J., 2019. Spermatozoa motility in bivalves: Signaling, flagellar beating behavior, and energetics. Theriogenology 136, 15–27. https://doi.org/10.1016/J.THERIOGENOLOGY.2019.06.025

Boulais, M., Soudant, P., Le Goïc, N., Quéré, C., Boudry, P., Suquet, M., 2017. ATP content and

 viability of spermatozoa drive variability of fertilization success in the Pacific oyster

 (Crassostrea gigas). Aquaculture 479, 114–119.

 https://doi.org/10.1016/j.aquaculture.2017.05.035

Boulais, M., Suquet, M., Arsenault-Pernet, E.J., Malo, F., Queau, I., Pignet, P., Ratiskol, D.,

 Grand, J. Le, Huber, M., Cosson, J., 2018. PH controls spermatozoa motility in the

 Pacific oyster (Crassostrea gigas). Biol Open 7.

 https://doi.org/10.1242/BIO.031427/259283/AM/PH-CONTROLS-SPERMATOZOA-

 MOTILITY-IN-THE-PACIFIC

Brown, V.M., Keim, B.D., Black, A.W., 2019. Climatology and Trends in Hourly Precipitation

 for the Southeast United States. J Hydrometeorol 20, 1737–1755.

 https://doi.org/10.1175/JHM-D-19-0004.1

Burchard, H., Schuttelaars, H.M., Ralston, D.K., 2018. Sediment Trapping in Estuaries. Annu.

 Rev. Mar. Sci 10, 371–95. https://doi.org/10.1146/annurev-marine-010816

Butts, I.A.E., Babiak, I., Ciereszko, A., Litvak, M.K., Słowińska, M., Soler, C., Trippel, E.A.,

 2011. Semen characteristics and their ability to predict sperm cryopreservation potential

 of Atlantic cod, Gadus morhua L. Theriogenology 75, 1290–1300.

 https://doi.org/10.1016/J.THERIOGENOLOGY.2010.11.044

Cosson, J., Groison, A.L., Suquet, M., Fauvel, C., Dreanno, C., Billard, R., 2008. Studying sperm

 motility in marine fish: an overview on the state of the art. Journal of Applied

 Ichthyology 24, 460–486. https://doi.org/10.1111/J.1439-0426.2008.01151.X

Cox, C., Mann, R.L., n.d. Temporal and spatial changes in fecundity of eastern oysters,

 Crassostrea virginica (Gmelin, 1791) in the James River, Virginia.

Dong, Q., Huang, C., Tiersch, T.R., 2005. Spermatozoal ultrastructure of diploid and tetraploid Pacific oysters. Aquaculture 249, 487–496. https://doi.org/10.1016/J.AQUACULTURE.2005.03.009

Eckelbarger, K.J., Davis, C. V., 1996a. Ultrastructure of the gonad and gametogenesis in the eastern oyster, Crassostrea virginica. II. Testis and spermatogenesis. Mar Biol 127, 89–96. https://doi.org/10.1007/BF00993648/METRICS

Eckelbarger, K.J., Davis, C. V., 1996b. Ultrastructure of the gonad and gametogenesis in the eastern oyster, Crassostrea virginica. I. Ovary and oogenesis. Mar Biol 127, 79–87. https://doi.org/10.1007/BF00993647/METRICS

Fabioux, C., Huvet, A., Le Souchu, P., Le Pennec, M., Pouvreau, S., 2005. Temperature and photoperiod drive Crassostrea gigas reproductive internal clock. Aquaculture 250, 458–470. https://doi.org/10.1016/j.aquaculture.2005.02.038

Gallager, S.M., Mann, R., 1986. Growth and survival of larvae of Mercenaria mercenaria (L.) and Crassostrea virginica (Gmelin) relative to broodstock conditioning and lipid content of eggs. Aquaculture 56, 105–121. https://doi.org/10.1016/0044-8486(86)90021-9

Gong, N., Yang, H., Zhang, G., Landau, B.J., Guo, X., 2004. Chromosome inheritance in triploid Pacific oyster Crassostrea gigas Thunberg. Heredity (Edinb) 93, 408–415. https://doi.org/10.1038/sj.hdy.6800517

Gregory, K.M., McFarland, K., Hare, M.P., 2023. Reproductive Phenology of the Eastern Oyster, Crassostrea virginica (Gmelin, 1791), Along a Temperate Estuarine Salinity Gradient. Estuaries and Coasts 46, 707–722. https://doi.org/10.1007/S12237-022-01163-W/TABLES/8

Guo, X., Debrosse, G.A., Allen, S.K., 1996. Aquaculture All-triploid Pacific oysters (Crassostrea gigas Thunberg) produced by mating tetraploids and diploids. Aquaculture 142, 149–161.

Guo, X., Wang, Y., Xu, Z., Yang, H., 2009. Chromosome set manipulation in shellfish. New Technologies in Aquaculture: Improving Production Efficiency, Quality and Environmental Management 165–194. https://doi.org/10.1533/9781845696474.1.165

Howard, D.W., Smith, C.S., Baldridge, M., Byrne, J. V, Gordon, W.G., 1983. Histological Techniques for Marine Bivalve Mollusks National Oceanic and Atmospheric Administration.

IPCC, 2022: Summary for Policymakers [H.-O. Pörtner, D.C. Roberts, E.S. Poloczanska, K. Mintenbeck, M. Tignor, A. Alegría, M. Craig, S. Langsdorf, S. Löschke, V. Möller, A. Okem (eds.)]. In: Climate Change 2022: Impacts, Adaptation and Vulnerability. Contribution of Working Group II to the Sixth Assessment Report of the Intergovernmental Panel on Climate Change [H.-O. Pörtner, D.C. Roberts, M. Tignor, E.S. Poloczanska, K. Mintenbeck, A. Alegría, M. Craig, S. Langsdorf, S. Löschke, V. Möller, A. Okem, B. Rama (eds.)]. Cambridge University Press, Cambridge, UK and New York, NY, USA, pp. 3–33, https://doi.org/10.1017/9781009325844.001

Kennedy, V.S., 1996. The ecological role of the eastern oyster, Crassostrea virginica, with remarks on disease. Oceanographic Literature Review 12, 1251.

Kennedy, V.S., Newell, R.I.E., Eble, A.F., 1996. The Eastern oyster: Crassostrea virginica. Maryland Sea Grant College.

Kime, D.E., Ebrahimi, M., Nystenb, K., Roelantsb, I., Rurangwab, E., Moorec, H.D.M., Ollevierb, F., 1996. Use of computer assisted sperm analysis (CASA) for monitoring the

effects of pollution on sperm quality of fish; application to the effects of heavy metals. Aquatic Toxicology 36, 223–237.

La Peyre, M.K., Marshall, D.A., and Sable, S.E., 2021, Oyster model inventory: Identifying critical data and modeling approaches to support restoration of oyster reefs in coastal U.S. Gulf of Mexico waters: U.S. Geological Survey Open-File Report 2021–1063, 40 p., https://doi.org/10.3133/ofr20211063.

Lango-Reynoso, F., Chávez-Villalba, J., Cochard, J.C., Le Pennec, M., 2000. Oocyte size, a means to evaluate the gametogenic development of the Pacific oyster, Crassostrea gigas (Thunberg). Aquaculture 190, 183–199. https://doi.org/10.1016/S0044-8486(00)00392-6

Leal Filho, W., Nagy, G.J., Martinho, F., Saroar, M., Erache, M.G., Primo, A.L., Pardal, M.A., Li, C., 2022. Influences of Climate Change and Variability on Estuarine Ecosystems: An Impact Study in Selected European, South American and Asian Countries. Int J Environ Res Public Health 19, 585. https://doi.org/10.3390/ijerph19010585

Loosanoff, V.L., Davis, H.C., 1952. Temperature requirements for maturation of gonads of northern oysters. Biol Bull 103, 80–96. https://doi.org/10.2307/1538408

López, A.G., Najjar, R.G., Friedrichs, M.A.M., Hickner, M.A., Wardrop, D.H., 2021. Estuaries as Filters for Riverine Microplastics: Simulations in a Large, Coastal-Plain Estuary. Front Mar Sci 8, 715924. https://doi.org/10.3389/FMARS.2021.715924/BIBTEX

Lowe, M.R., Sehlinger, T., Soniat, T.M., Peyre, M.K. La, 2017. Interactive Effects of Water Temperature and Salinity on Growth and Mortality of Eastern Oysters, Crassostrea virginica : A Meta-Analysis Using 40 Years of Monitoring Data. J Shellfish Res 36, 683–697. https://doi.org/10.2983/035.036.0318

Marshall, D.A., Coxe, N.C., La Peyre, M.K., Walton, W.C., Rikard, F.S., Pollack, J.B., Kelly, M.W., La Peyre, J.F., 2021. Tolerance of northern Gulf of Mexico eastern oysters to chronic warming at extreme salinities. J Therm Biol 100, 103072. https://doi.org/10.1016/j.jtherbio.2021.103072

Moore, J.F., Pine, W.E., Frederick, P.C., Beck, S., Moreno, M., Dodrill, M.J., Boone, M., Sturmer, L., Yurek, S., 2020. Trends in Oyster Populations in the Northeastern Gulf of Mexico: An Assessment of River Discharge and Fishing Effects over Time and Space. Marine and Coastal Fisheries 12, 191–204. https://doi.org/10.1002/MCF2.10117

Myers, J.N., Nichols, Z.G., Abualreesh, M.H., El Husseini, N., Taylor, Z.A., Coogan, M.P., Gurbatow, J., Vo, K.M., Zadmajid, V., Chatakondi, N., Dunham, R.A., Butts, I.A.E., 2020. Impact of sperm density on hatch success for channel catfish (Ictalurus punctatus) ♀ × blue catfish (Ictalurus furcatus) ♂ hybrid production. Aquaculture 521, 735024. https://doi.org/10.1016/J.AQUACULTURE.2020.735024

National Marine Fisheries Service, 2022. Fisheries of the United States. (2020). U.S. Department of Commerce, NOAA Current Fishery Statistics No. 2020. https://www.fisheries.noaa.gov/national/sustainable-fisheries/fisheries-united-states (accessed 16 August 2023)

Nell, J.A., 2002. Farming triploid oysters. Aquaculture 210, 69–88. https://doi.org/10.1016/S0044-8486(01)00861-4

Nelson, T.C., 1928. Relation of Spawning of the Oyster to Temperature. Ecology 9, 145–154. https://doi.org/10.2307/1929351

Nichols, Z.G., Rikard, S., Mohammad, S., Alavi, H., Walton, W.C., Buttsid, I.A.E., 2021. Regulation of sperm motility in Eastern oyster (Crassostrea virginica) spawning naturally in seawater with low salinity. https://doi.org/10.1371/journal.pone.0243569

NOAA, 2021. Why are Estuaries Important? [WWW Document]. The Economy and Environment National Ocean Service website. URL https://oceanservice.noaa.gov/education/tutorial_estuaries/est02_economy.html (accessed 10.4.23).

[Database] NOAA Fisheries Office of Science and Technology, Commercial Landings Query, www.fisheries.noaa.gov/foss (accessed 16 August 2023)

Piferrer, F., Beaumont, A., Falguière, J.-C., Flajšhans, M., Haffray, P., Colombo, L., 2009. Polyploid fish and shellfish: Production, biology and applications to aquaculture for performance improvement and genetic containment. Aquaculture 293, 125–156. https://doi.org/10.1016/j.aquaculture.2009.04.036

Prein, A.F., Rasmussen, R.M., Ikeda, K., Liu, C., Clark, M.P., Holland, G.J., 2017. The future intensification of hourly precipitation extremes. Nat Clim Chang 7, 48–52. https://doi.org/10.1038/nclimate3168

Quintana, R., Burnside, W.M., Supan, J.E., Lynn, J.W., Tiersch, T.R., 2011. Rapid Estimation of Gonad-to-Body Ratio in Eastern Oysters by Image Analysis. N Am J Aquac 73, 451–455. https://doi.org/10.1080/15222055.2011.630258

Rouleau, T., Colgan, C.S., Adkins, J., Castelletto, A., Dirlam, P., Lyons, S., Stevens, H., 2021. The Economic Value of America's Estuaries: 2021 Update.

Rurangwa, E., Kime, D.E., Ollevier, F., Nash, J.P., 2004. The measurement of sperm motility and factors affecting sperm quality in cultured fish. Aquaculture 234, 1–28. https://doi.org/10.1016/J.AQUACULTURE.2003.12.006

Rurangwa, E., Volckaert, F.A.M., Huyskens, G., Kime, D.E., Ollevier, F., 2001. Quality control of refrigerated and cryopreserved semen using computer-assisted sperm analysis (CASA), viable staining and standardized fertilization in African catfish (Clarias gariepinus). Theriogenology 55, 751–769. https://doi.org/10.1016/S0093-691X(01)00441-1

Shumway, S.,1996, Natural environmental factors. In: Kennedy, V.S., Newell, R.I.E. and Eble, A.F., Eds., The Eastern Oyster Crassostrea virginica. Maryland Sea Grant College, College Park, 467-513

Song, Y.P., Suquet, M., Quéau, I., Lebrun, L., 2009. Setting of a procedure for experimental fertilisation of Pacific oyster (Crassostrea gigas) oocytes 287, 311–314. https://doi.org/10.1016/j.aquaculture.2008.10.018

Spilke, J., Piepho, H.P., Hu, X., 2005. Analysis of Unbalanced Data by Mixed Linear Models Using the mixed Procedure of the SAS System. J Agron Crop Sci 191, 47–54. https://doi.org/10.1111/J.1439-037X.2004.00120.X

Suquet, M., Labbe, C., Brizard, R., Donval, A., Le Coz, J.R., Quere, C., Haffray, P., 2010. Changes in motility, ATP content, morphology and fertilisation capacity during the movement phase of tetraploid Pacific oyster (Crassostrea gigas) sperm. Theriogenology 74, 111–117. https://doi.org/10.1016/j.theriogenology.2010.01.021

Thompson, R.J., Newell, R.I.E., Kennedy, V.S., Mann, R., 1996. Reproductive processes and early development, in: The Eastern Oyster Crassostrea Virginica. Maryland Sea Grant College, College Park, pp. 335–370.

Tomkiewicz, J., Kofoed, T.M.N., Pedersen, J.S., 2011. Assessment of testis development during induced spermatogenesis in the European eel Anguilla Anguilla. Marine and Coastal Fisheries 3, 106–118. https://doi.org/10.1080/19425120.2011.556902

USEPA. 1999. Ecological Condition of Estuaries in the Gulf of Mexico. EPA 620-R-98- 004. U.S. Environmental Protection Agency, Office of Research and Development, National Health and Environmental Effects Research Laboratory, Gulf Ecology Division, Gulf Breeze, Florida.

Vignier, J., Volety, A.K., Rolton, A., Le Goïc, N., Chu, F.-L.E., Robert, R., Soudant, P., 2017. Sensitivity of eastern oyster (Crassostrea virginica) spermatozoa and oocytes to dispersed oil: Cellular responses and impacts on fertilization and embryogenesis. Environmental Pollution 225, 270–282. https://doi.org/10.1016/j.envpol.2016.11.052

Wallace, R.K., Waters, P., Rikard, F.S., 2008. Oyster Hatchery Techniques.

Wang, Z., Boyer, T., Reagan, J., Hogan, P., 2023. Upper-Oceanic Warming in the Gulf of Mexico between 1950 and 2020. J Clim 36, 2721–2734. https://doi.org/10.1175/JCLI-D-22-0409.1

Yang, H., Guo, X., Scarpa, J., 2019. Tetraploid Induction and Establishment of Breeding Stocks for All-Triploid Seed Production. EDIS 2019. https://doi.org/10.32473/edis-fa215-2019

Yang, H., Simon, N., Sturmer, L.N., 2018. Production and Performance of Triploid Oysters for Aquaculture: FA208, 7/2018. EDIS 2018. https://doi.org/10.32473/EDIS-FA208-2018
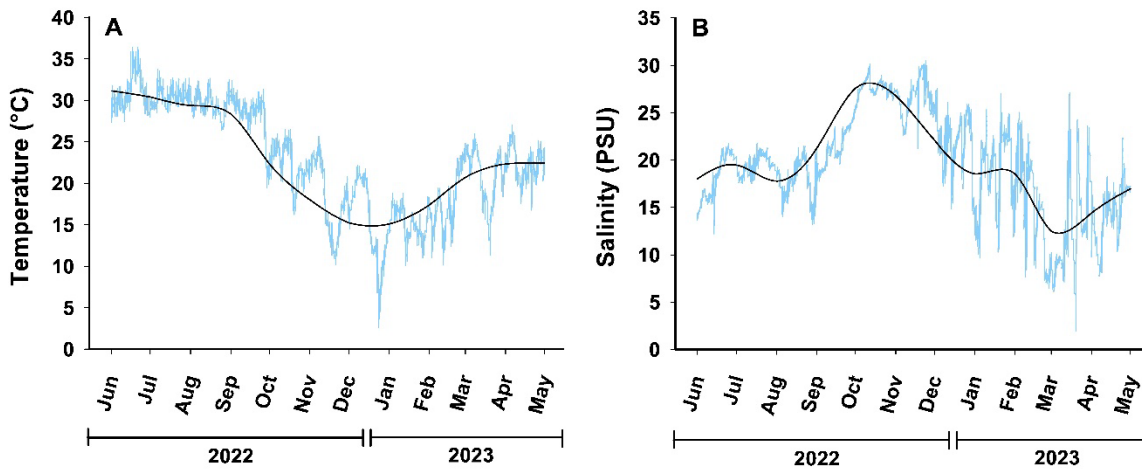
Figure 2.1 Average hourly water temperature (°C; A) and salinity (PSU; B) in Grand Bay AL (30.3749090ºN, -88.3145984ºW) from June 2022 to May 20223. Black line represents monthly mean.
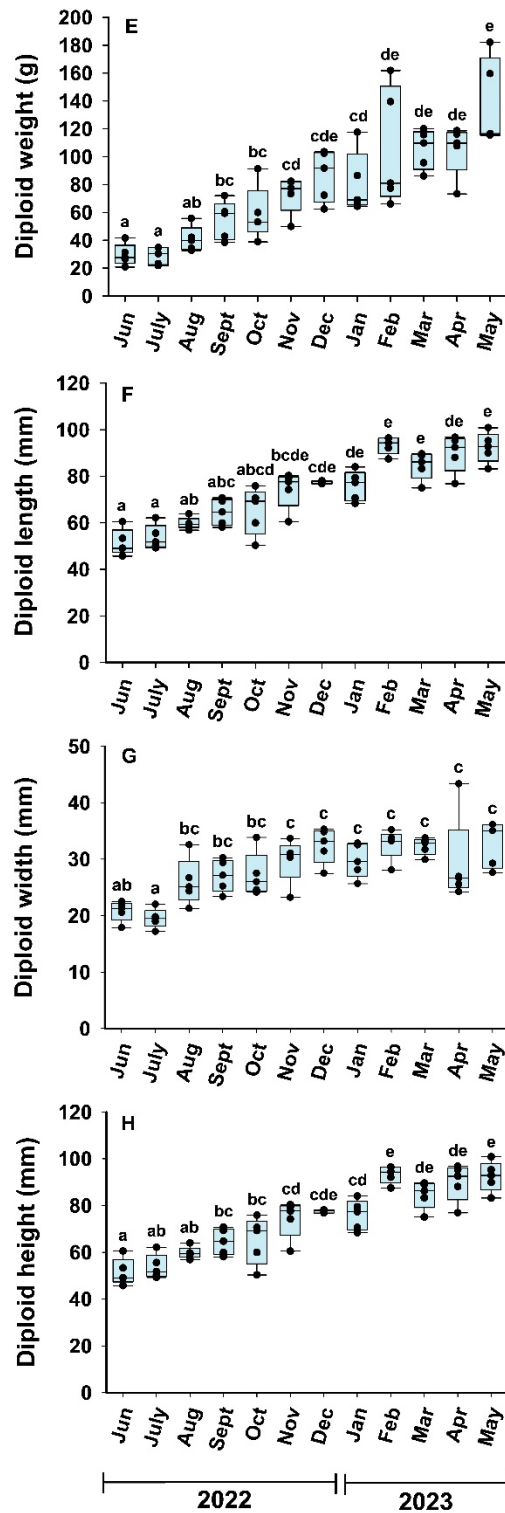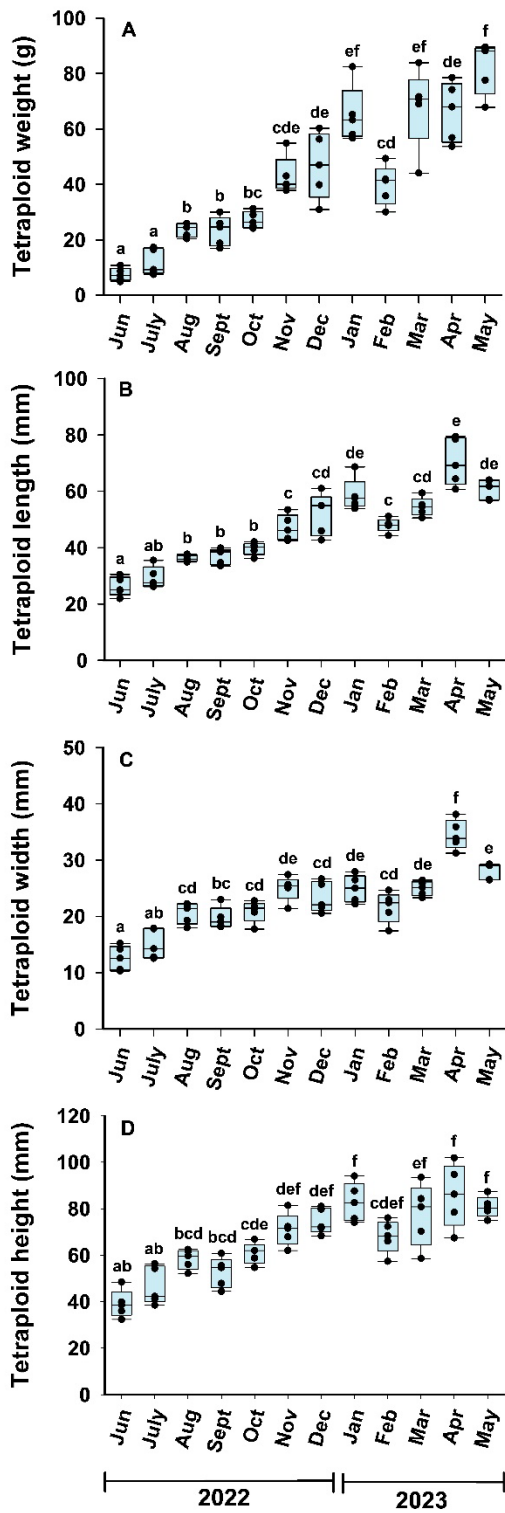
Figure 2.2 Effect of month on the changes in weight and shell morphology in tetraploid (A-D) and diploid (E-H) Eastern oyster (*Crassostrea virginica*). One-way ANOVA was used to compare monthly weight, shell length, height, and width within each ploidy over an annual cycle. Box heights indicate interquartile range, horizontal line within box indicates median and mean, whiskers show minimum and maximum value within data, and dots represent individual values. Means were contrasted using the Tukey-Kramer method and months with same letters were not significantly different (P > 0.05).
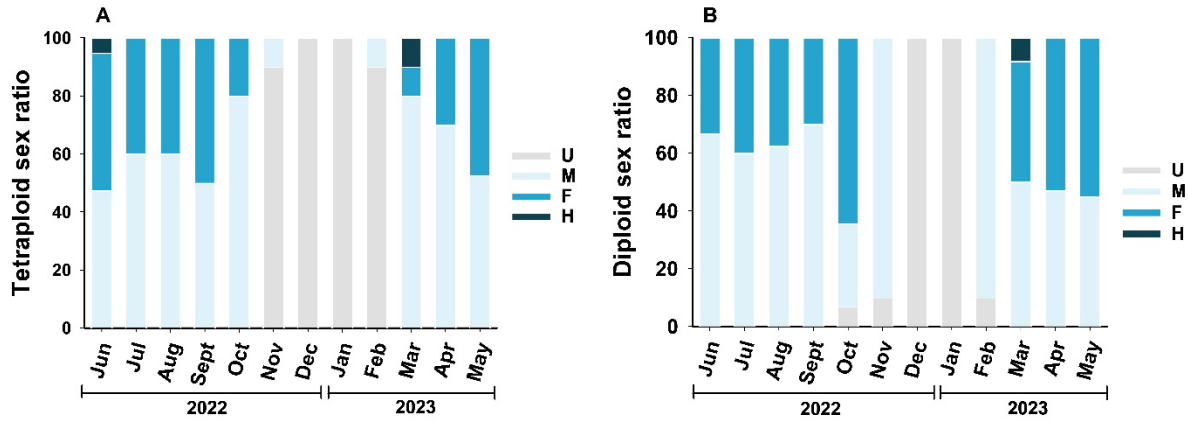
Figure 2.3 Proportions of tetraploid (A) and diploid (B) Eastern oyster (*Crassostrea virginica*) in each genotypic sex category from June 2022 to May 2023. U = unidentified, M = male, F = female, H = hermaphrodite.
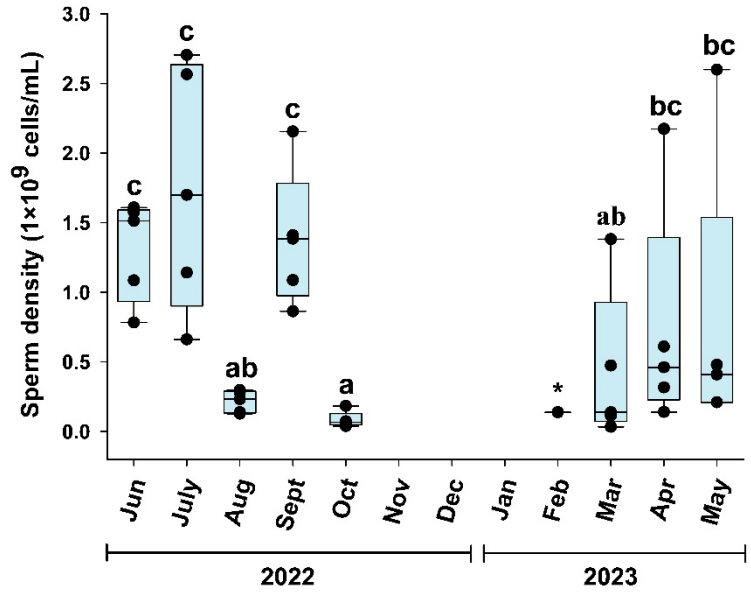
Figure 2.4 Tetraploid Eastern oyster (*Crassostrea virginica*) sperm density over an annual cycle (June 2022 - May 2023). One-way ANOVA was used to compare density between each month of a gametogenic cycle. Box heights indicate interquartile range, horizontal line within box indicates median and mean, whiskers show minimum and maximum value within data, and dots represent individual values. Means were contrasted using the Tukey-Kramer method and months with same letters were not significantly different ($P > 0.05$). Asterisk represents one male found in February, excluded from statistical analysis.
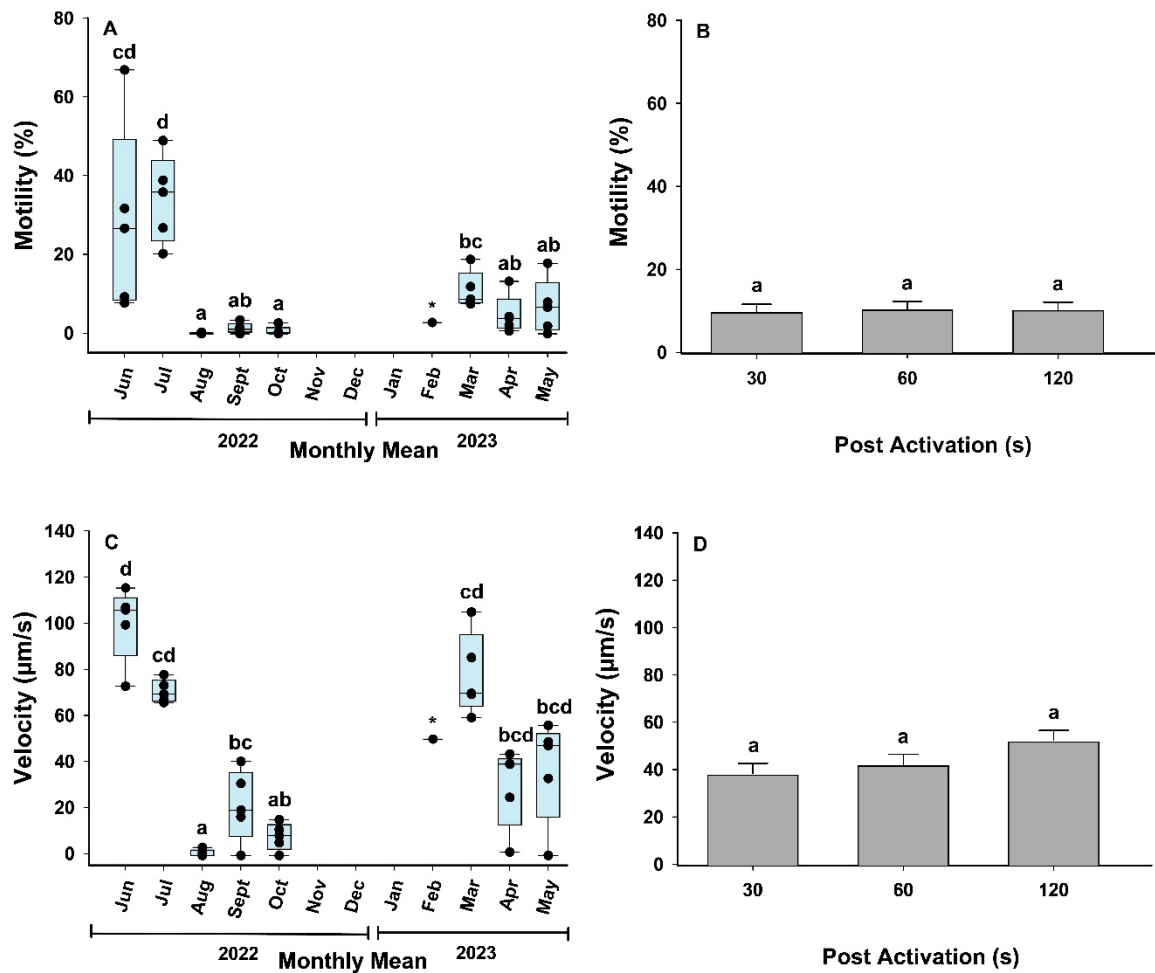
Figure 2.5 Effect of month on sperm kinematics in tetraploid Eastern oyster (*Crassostrea virginica*). Computer Assisted Sperm Analysis was used to determine the impact of month on percent motility (A-B) and sperm curvilinear velocity (VCL; C-D) at 30, 60, and 120 s post activation. Main effects were interpreted as interactions were non-significant (A-D). Box heights indicate interquartile range, horizontal line within box indicates median and mean, whiskers show minimum and maximum value within data, and dots represent individual values (A C). Means were contrasted using the Tukey-Kramer method and months with same letters were not

significantly different (P > 0.05). Asterisk represents one male found in February, excluded from statistical analyses.
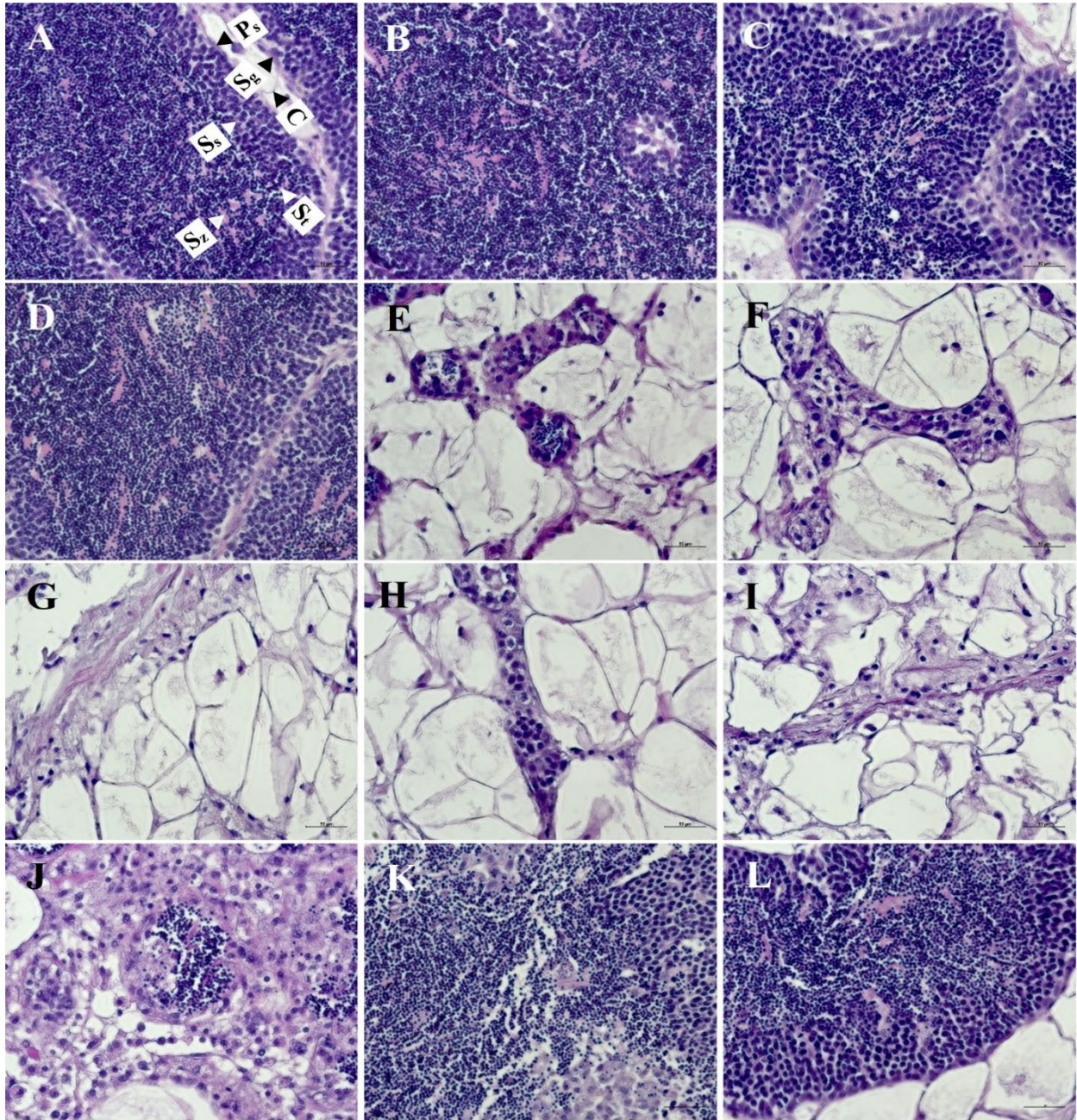
Figure 2.6 Digital Images (scale bar = 50 µm) of histological samples for male tetraploid Eastern oyster (*Crassostrea virginica*) over an annual cycle. The sampling period included June to August 2022 (A-C), September to November 2022 (D-F), December 2022 to February 2023 (G-I), and March to May 2023 (J-L). Arrows indicating cell development (A) include connective tissue and

excluded area (C), spermatogonia (S_g), primary spermatocytes (P_s), secondary spermatocytes (S_s), spermatids (S_t) and spermatozoa (S_z).
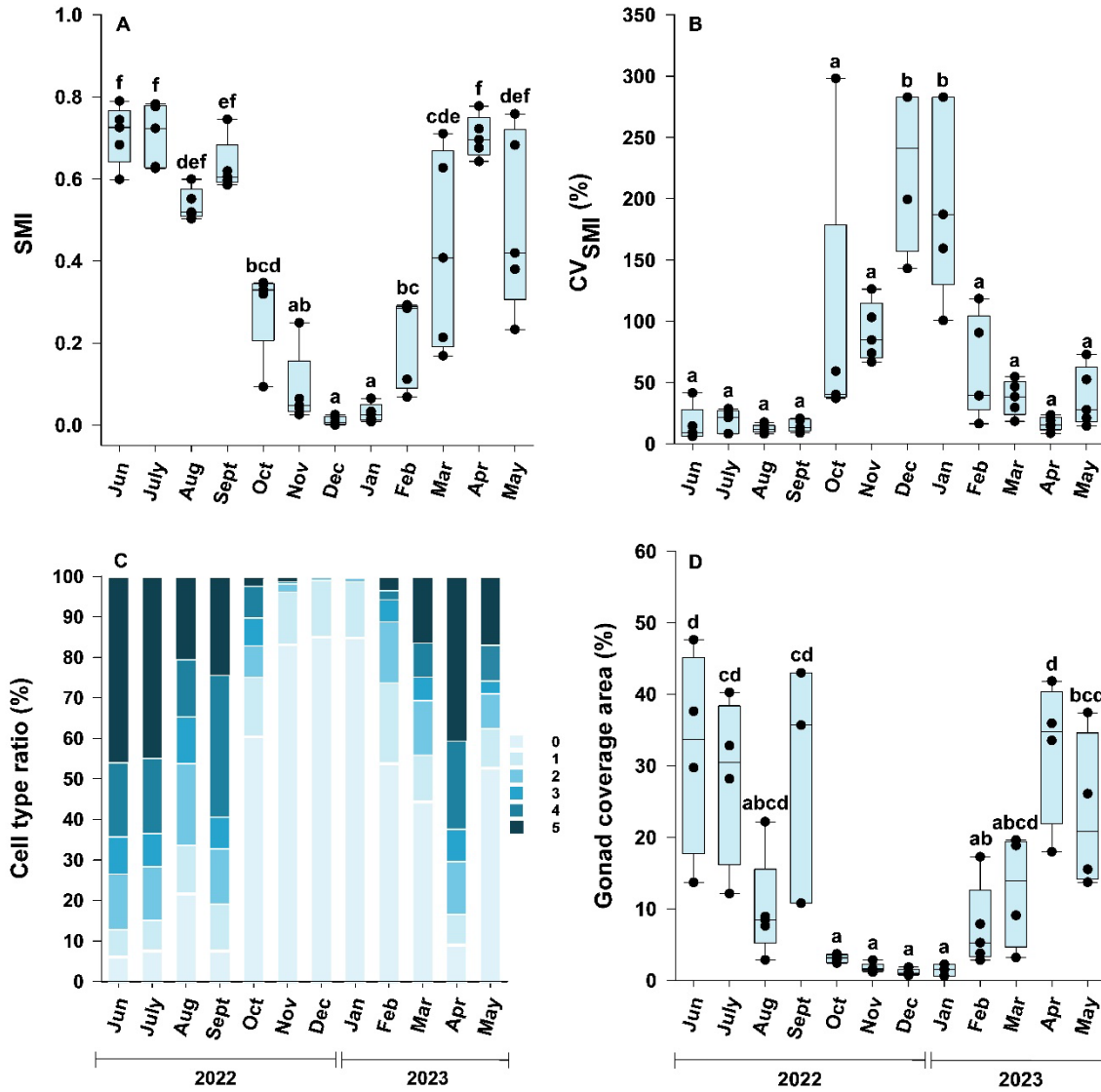
Figure 2.7 Effect of month on Spermatogenic Maturity Index (SMI; A), the male-to-male variation in SMI (measured as coefficient of variation; CV; B), cell type ratio (C), and gonad coverage area (D) for male tetraploid Eastern oyster (*Crassostrea virginica*) over a one-year sampling period. Cell type is represented graphically, where Connective tissue = 0, spermatogonia = 1, primary spermatocytes = 2, secondary spermatocytes = 3, spermatids = 4, and spermatozoa = 5. One-way ANOVA was used to compare SMI, the CV for SMI, and gonad coverage area, independently, between months over an annual cycle. Box heights indicate interquartile range, horizontal line

within box indicates median and mean, whiskers show minimum and maximum value within data, and dots represent individual values. Means were contrasted using the Tukey-Kramer method and months with same letters were not significantly different ($P > 0.05$).
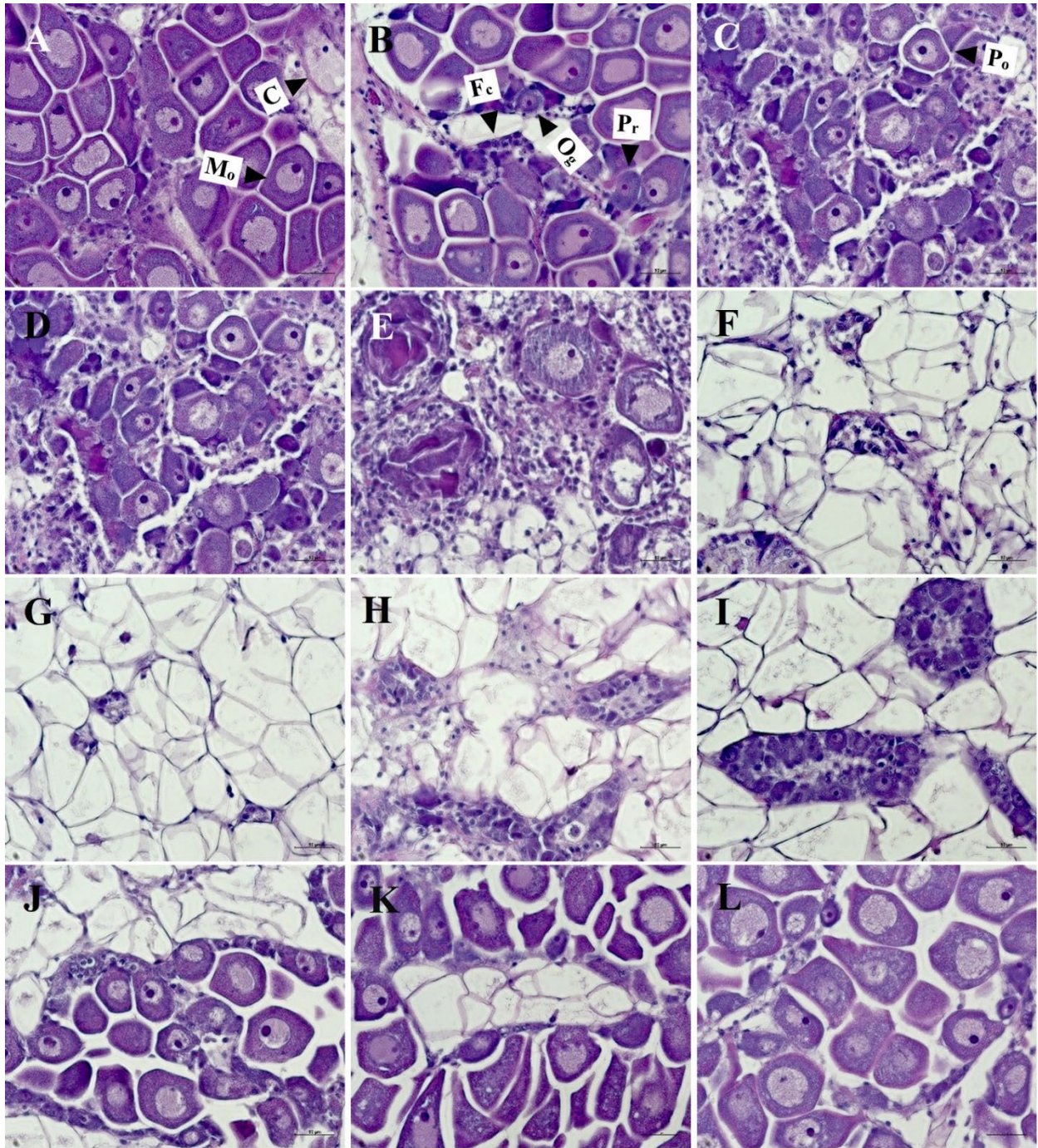
Figure 2.8 Digital Images (scale bar = 50 μm) of histological samples of female diploid Eastern oyster (*Crassostrea virginica*) over an annual cycle. The sampling period included June to August 2022 (A-C), September to November 2022 (D-F), December 2022 to February 2023 (G-I), and

March to May 2023 (J-L). Arrows indicating cell development (A-C) include connective tissue and excluded area (C), follicular cells (F_c), oogonia (O_g), previtellogenic oocyte (P_r), post-vitellogenic oocytes (P_o), and mature oocytes (M_o).
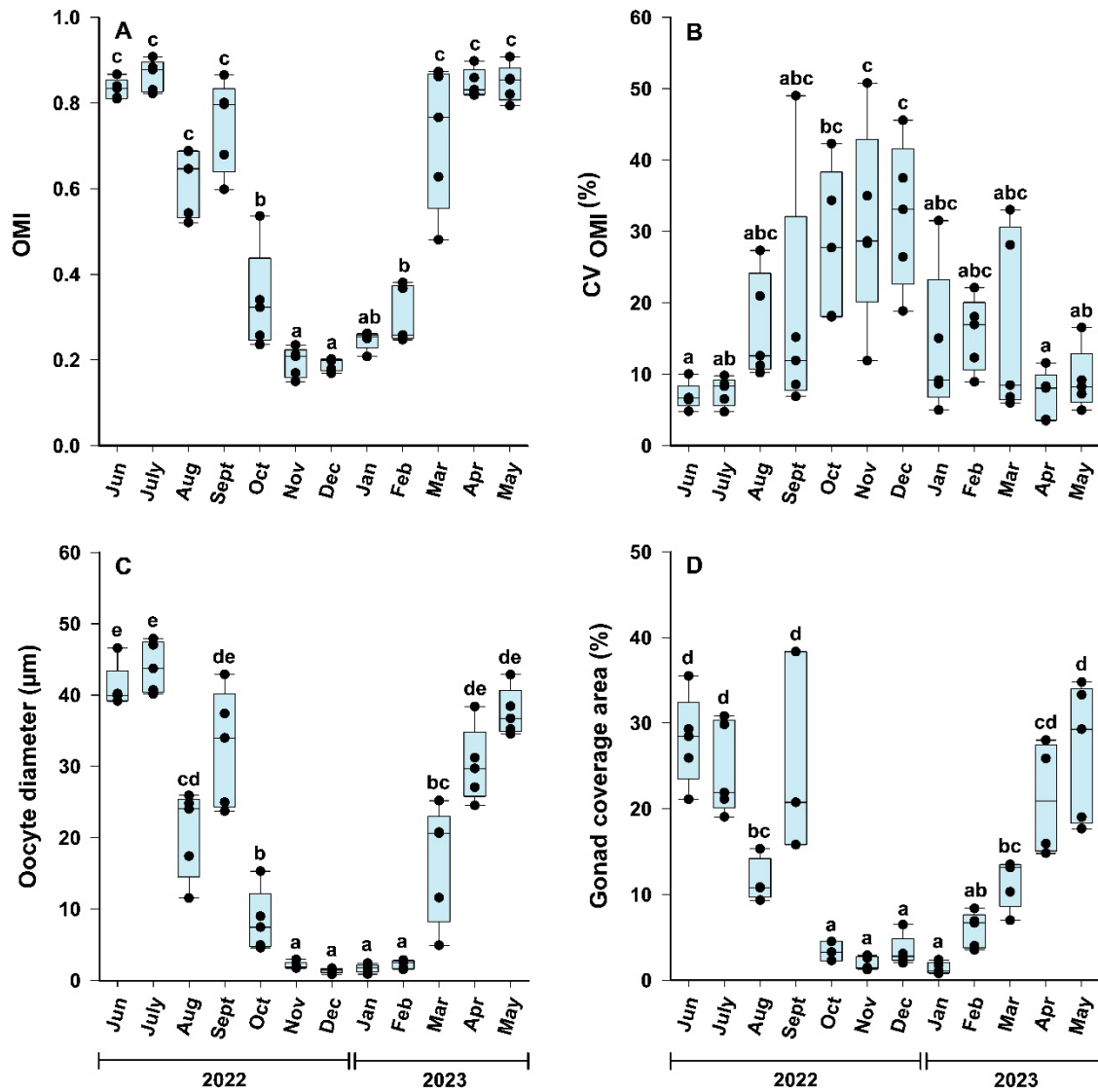
Figure 2.9. Effect of month on Oogenesis Maturity Inex (OMI; A), CV of the OMI(B), Oocyte Diameter (C), and Gonad coverage area (D) for female diploid Eastern oyster (*Crassostrea virginica*) over an annual cycle. One-way ANOVA was used to compare each trait between months over a one-year gametogenic cycle. Box heights indicate interquartile range, horizontal line within box indicates median and mean, whiskers show minimum and maximum value within data, and dots represent individual values. Means were contrasted using the Tukey-Kramer method and months with same letters were not significantly different (P > 0.05).

Table 2.1 Tissue area fraction calculations and Spermatogenesis Maturity Index (SMI) utilizing cell types from histological images of tetraploid Eastern oyster (*Crassostrea virginica*) and point counts (n) per tissue category (i). The SMI is the product of the weighted factor (w) and estimated F. Cell types of spermatogonia (Sg), primary spermatocytes (Ps), secondary spermatocytes (S), spermatids (St) and Spermatozoa (Sz); C = Connective tissue).

| Cell Type | i | n_i | Area fraction calculation | | SMI calculation | |
			$n_i/n_{total}-n_{1)}$	F	w	F x W
C	0	8				
S_g	1	2	2/(48-8)	0.050	0.00	0
P_s	2	7	7/(48-8)	0.175	0.25	0.044
S_s	3	3	3/(48-8)	0.075	0.50	0.038
S_t	4	13	13/(48-8)	0.325	0.75	0.425
S_z	5	15	15/(48-8)	0.375	1.00	0.375
Total		48		1.000		0.882

Table 2.2 Tissue area fraction calculations and Oogenesis Maturity Index (OMI) utilizing cell types from histological images of diploid Eastern oyster (*Crassostrea virginica*) and point counts (n) per tissue category. The OMI is the product of the weighted factor (w) and estimated F. Cell types of follicular cells (Fc), oogonia (Og), previtellogenic oocytes (Pr), post- vitellogenic oocytes (Po) and mature oocytes (Mo); C = Connective tissue).

| Cell Type | i | n_i | Area fraction calculation | | OMI calculation | |
			$n_i/n_{total}-n_i)$	F	w	F x W
C	0	5				
F_c	1	5	5/(30-5)	0.20	0.00	0
O_g	2	2	2/(30-5)	0.08	0.25	0.02
P_r	3	1	1/(30-5)	0.04	0.50	0.02
P_o	4	6	6/(30-5)	0.24	0.75	0.18
M_o	5	11	11/(30-5)	0.44	1.00	0.44
Total		30		1.00		0.66